

Zinc complexes supported by multidentate aminophenolate ligands: synthesis, structure and catalysis in ring-opening polymerization of *rac*-lactide†

Liyang Wang and Haiyan Ma*

Received 1st April 2010, Accepted 27th May 2010

First published as an Advance Article on the web 26th July 2010

DOI: 10.1039/c0dt00250j

Monomeric zinc silylamido and ethyl complexes bearing tetradentate aminophenolato ligands [(DNNO)ZnR] ($D = \text{NMe}_2$, OMe; $R = \text{N}(\text{SiMe}_3)_2$ (**1–5**, **8**), Et (**6**, **7**, **9**, **10**)), were isolated from the reaction of $\text{Zn}[\text{N}(\text{SiMe}_3)_2]_2$ or ZnEt_2 and one equivalent of aminophenols {aryl- $\text{CH}_2\text{N}[(\text{CH}_2)_2\text{NMe}_2]\text{CH}_2$ -phenol} in moderate to high yields. The monomeric nature of these complexes was further confirmed by X-ray diffraction studies of silylamido complexes **1**, **3** and ethyl complexes **7**, **9**, **10**. The methoxy or *N,N*-dimethylamino group of the aryl unit does not coordinate with the metal center in the solid state, only the remaining three donors of the ligand and silylamido or ethyl group interact with zinc center constructing a distorted tetrahedral coordination geometry at the metal center. All these zinc complexes efficiently initiated the ring-opening polymerization of *rac*-lactide, and the polymerization runs were better controlled in the presence of isopropanol, giving atactic PLAs end-capped with isopropyl ester and hydroxyl groups. The structure of the ancillary ligands showed some influence on the catalytic activity and selectivity of the corresponding zinc complexes. The introduction of bulky *ortho*-substituents on the phenoxy unit resulted in a decrease of the polymerization rate, whereas the isotactic dyad selectivity in the ROP of *rac*-lactide was enhanced.

Introduction

Poly(lactide) (PLA), prepared from natural renewable resources has recently gained much attention due to its biodegradable and biocompatible nature, and suitable properties as a potential alternative to polyolefins.^{1–4} Nowadays, methods for preparing high molecular weight poly(lactides) generally rely on the controlled ring-opening polymerization (ROP) of lactides initiated by well-defined metal complexes. Systematic mechanistic studies have demonstrated the influence both of the initiating group and of the ancillary ligand architecture on polymerization control, reaction rate and/or stereoselectivity during the polymerization process.^{5,6}

Stereocontrolled polymerizations have been observed by using aluminium initiators with salen-type ligands, and excellent isotactic stereospecificity can be obtained in the ROP of *rac*-lactide *via* either enantiomorphic site control^{7–12} or a chain-end control mechanism.^{13–20} The catalytic activities of these aluminium complexes are generally low and the polymerization runs had to be carried out at high temperature over a relatively long period of time. Rare-earth metal complexes are highly active for ROP of *rac*-lactide, in some cases showing significant preference for heterotactic dyad enchainment.^{21–28} When regarding possible incorporation of trace amount of metal residues in the obtained polymer, initiators consisting of biocompatible metals such as

zinc are therefore much preferred. In general, zinc complexes are efficient initiators for the ring-opening polymerization of lactide,^{29–32} but lacking satisfied isotactic selectivity and producing mainly heterotactic or atactic poly(lactides).^{33–42} Among them, zinc complexes with β -diketiminato, phenoxy-imine, phenoxy-amine have been extensively developed (Chart 1). Coates and co-workers synthesized zinc complexes bearing sterically demanding achiral β -diketiminato ligands (**A**), which initiated *rac*-lactide polymerization to afford heterotactic PLA *via* a chain-end control mechanism. In particular, the authors found that subtle modifications of steric bulkiness of the *N*-aryl substituents of β -diketiminato ligands resulted in dramatic effects on stereoselectivity (P_r could be improved to 0.94).³⁴ Chisholm reported that zinc silylamido complex ligated with phenoxy-imine ligand **B** catalyzed the polymerization of *rac*-lactide to give atactic poly(lactide).⁴² Lin *et al.* introduced zinc alkoxide complex supported by mono-methylether salen-type ligand **C** for the polymerization of *rac*-lactide to afford heterotactic predominant PLA with $P_r = 0.75$; meanwhile, a magnesium analogue containing the same ligand gave isotactic-enriched PLA with $P_m = 0.67$.³⁶ Further investigation showed that zinc alkoxide complexes supported by phenoxy-imine-amine ligands **D** proved highly heterotactic selective ($P_r = 0.91$) for ROP of *rac*-lactide in CH_2Cl_2 at low temperature.³⁹ Hillmyer and Tolman reported the highly active zinc ethoxide complexes derived from phenoxydiamine ligands **E**, which were observed to initiate rapid polymerization of *rac*-lactide at a high initial monomer-to-catalyst ratio of 1500, yielding PLAs with average molecular weight as large as 130 kg mol^{-1} .²⁹ Very recently, Mehrkhodavandi described some unusually stable chiral zinc ethyl complexes; among them, complexes supported by ligands **F** initiated *rac*-lactide polymerization to give PLA with $P_m = 0.54$.⁴³

Due to the divalent nature of the zinc ion, monoanionic ligands were utilized throughout to construct complexes of the

Laboratory of Organometallic Chemistry, East China University of Science and Technology, 130 Meilong Road, Shanghai, 200237, People's Republic of China. E-mail: haiyanma@ecust.edu.cn (H. Ma); Fax: +86 21 64253519; Tel: +86 21 64253519

† Electronic supplementary information (ESI) available: Variable-temperature ¹H NMR spectra of **10**, ¹H NMR spectra of active *rac*-lactide oligomer by **1**/ⁱPrOH, the complex **1** and the ligand **L¹H**, ¹H NMR trace spectra of reaction between complex **9** and isopropanol. CCDC reference numbers 772262–772266 for **1**, **3**, **7**, **9** and **10**. For ESI and crystallographic data in CIF or other electronic format see DOI: 10.1039/c0dt00250j

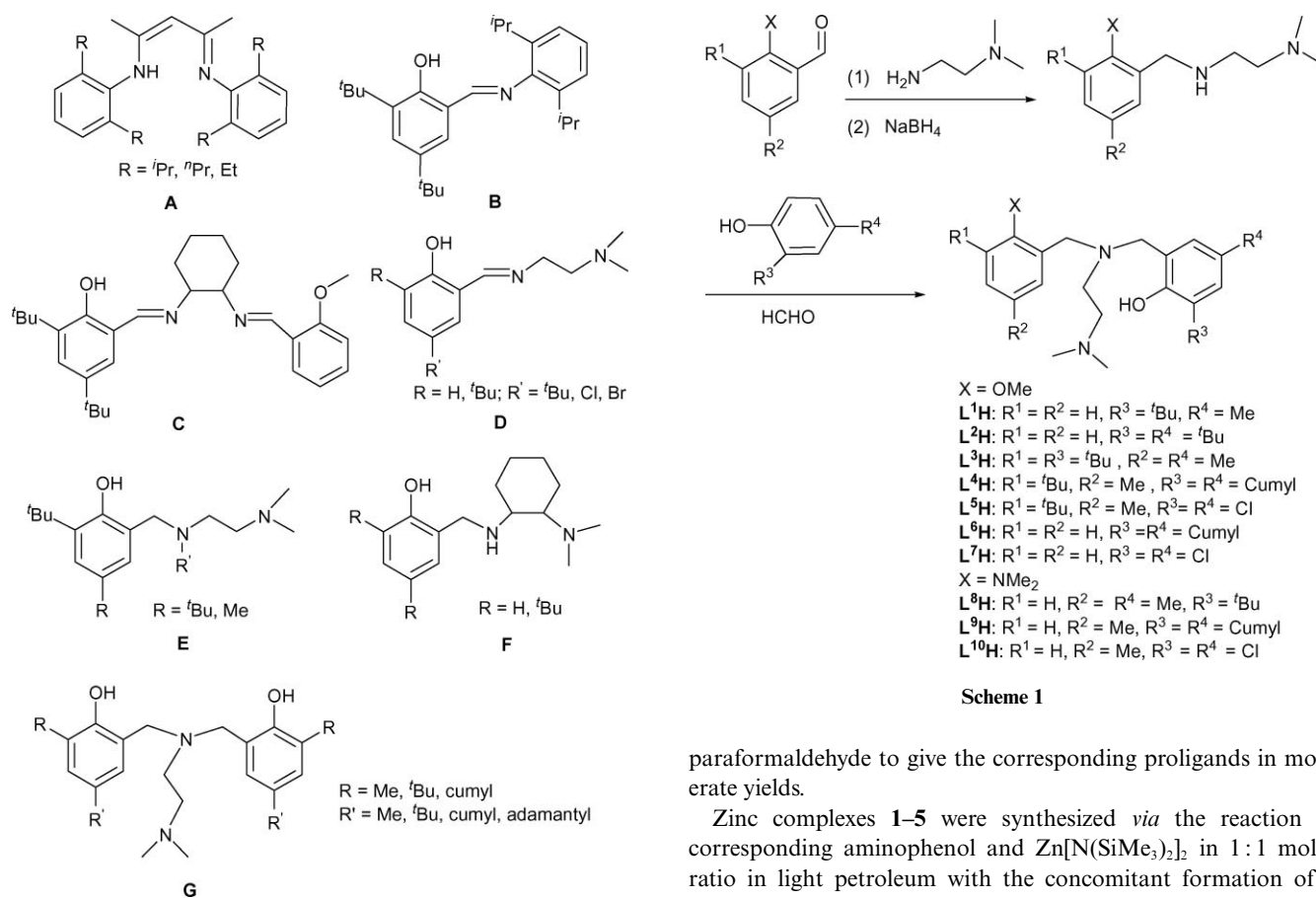


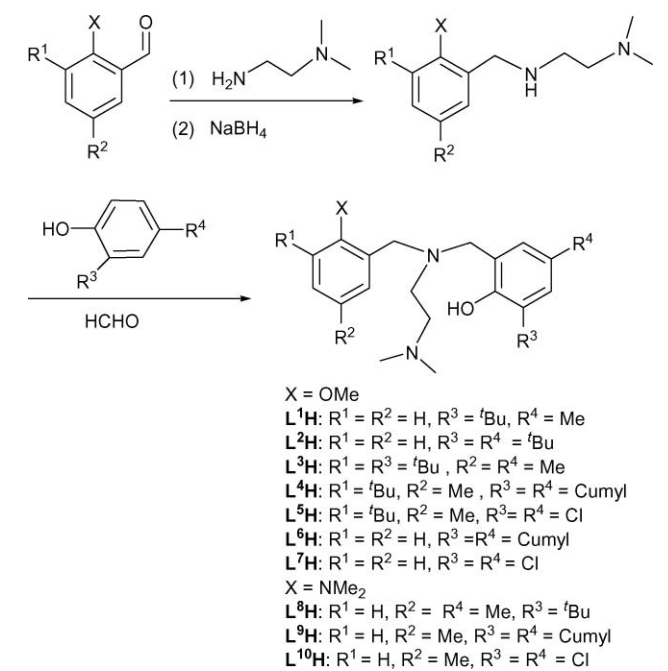
Chart 1

form $L_n\text{ZnX}$ (where L_n represents a multidentate monoanionic ligand, X is a group capable of initiating polymerization or can be converted to such a group). However, structural features of ancillary ligands capable of governing isotactic stereocontrol during the ROP of lactide by zinc complexes are still uncertain rather than uncovered. Crucial factors in the polymerization process such as activity and stereoselectivity need to be further studied for well-defined zinc complexes. Herein, we report the synthesis and lactide polymerization investigation of a series of zinc complexes bearing monoanionic claw-type aminophenolate ligands with the aim to construct an asymmetric coordination environment around the metal center for selective monomer recognition. Nevertheless, zinc complexes with similar bis(phenolate) ligand **G** hardly initiated the polymerization of cyclic esters.⁴⁴

Results and discussion

Synthesis and spectroscopic studies

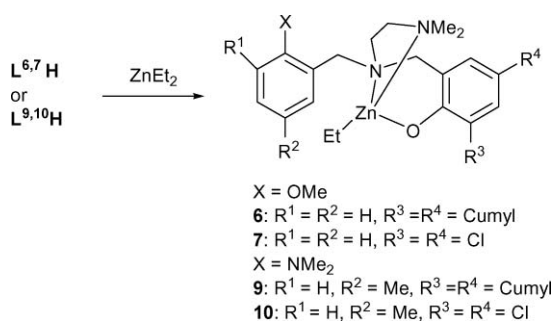
The tetradentate phenol proligands (**L¹⁻¹⁰H**) were prepared *via* three-step reactions as illustrated in Scheme 1. The condensation reaction of arylaldehydes with *N,N*-dimethylethylenediamine in methanol afforded the corresponding Schiff-base compounds which were sequentially reduced to amines without further purification; the crude amines were then exposed to a modified Mannich reaction with substituted phenols in the presence of



Scheme 2

paraformaldehyde to give the corresponding proligands in moderate yields.

Zinc complexes **1-5** were synthesized *via* the reaction of corresponding aminophenol and $\text{Zn}[\text{N}(\text{SiMe}_3)_2]_2$ in 1 : 1 molar ratio in light petroleum with the concomitant formation of 1 equiv. of $\text{HN}(\text{SiMe}_3)_2$ at room temperature. Analytically pure complexes **1-5** were isolated from toluene or hexane as colorless, air/moisture sensitive crystalline solids in 61–75% yields after work-up (Scheme 2). In the case of **L⁶H** or **L⁷H**, a similar approach only acquired white powders which were very poorly soluble in common solvents such as light petroleum, aromatic solvents, and decomposed in methylene dichloride and THF. To overcome the problem of dissolvability, one equiv. of **L⁶H** or **L⁷H** was treated with diethyl zinc to afford zinc ethyl complexes **6** and **7** by ethane elimination reaction in almost quantitative yields (Scheme 3). Zinc complex **8** containing an aryl-*N,N*-dimethylamino group could be synthesized similarly as complexes **1-5** *via* amine elimination reaction, but analogous complexes with either cumyl or chloro substituents could not be prepared



Scheme 3

due to poor solubility in common hydrocarbon solvents, thus corresponding zinc ethyl complexes **9** and **10** were obtained from the reaction of aminophenols **L⁹H**, **L¹⁰H** with diethyl zinc.

The stoichiometric structures of complexes **1–10** were further confirmed on the basis of ^1H and ^{13}C NMR spectroscopy as well as elemental analysis. In the ^1H NMR spectrum of complex **1** in C_6D_6 , the two protons of each methylene in the $\text{Ar}-\text{CH}_2-\text{N}$ units are inequivalent and give rise to two doublets as compared to the singlet in the free ligand, indicating a rigid configuration in solution. Similar phenomena were also displayed in the proton NMR spectra of the remaining zinc complexes except for complex **4**, where two doublets at 4.33, 3.28 ppm with coupling constant of $^2J = 12.8$ Hz as well as one singlet accounting for two protons at 4.11 ppm are displayed. It is worth noting that the methylene resonances of the bridging unit ($\text{NCH}_2\text{CH}_2\text{N}$) in these zinc complexes exhibit unexpected features. Besides the unidentifiable coupling modes, the signal of one methylene proton shifts upfield significantly ($\Delta\delta = 0.5\text{--}0.8$ ppm for silylamido complexes), while the remainder are at the same positions as those of the free ligand. By referring the result of X-ray diffraction studies, we suggest that it is most likely due to some specific shielding effect of the aromatic rings.

To better understand the coordination environment around the zinc center in complexes **1–10**, chemical shifts of representative donor groups are summarized in Table 1. It is found that the sharp resonance assignable to $\text{Ar}-\text{OCH}_3$ in complexes **1–7** hardly changes when compared to that of the corresponding free ligand. However, the resonance assignable to the six protons of the dimethylamino group either splits into two peaks or still displays as a singlet, but both along with significant broadening. All these suggest that in complexes **1–7** the nitrogen atom of

the dimethylamino group should take part in the coordination with the zinc center; the coordination of the methoxy group is however inconclusive. Most likely the same structure features are maintained in solution as they are in the solid state (*vide post*). The non-coordination mode of the methoxy group to the metal center was also observed for zinc complexes bearing a mono-methylether Salen-type ligand³⁶ as well as ether-substituted β -diketiminato ligands.³⁷

The alteration of aryl-methoxy group with dimethylamino in complex **8** does not change the coordination fashion, as similar features mentioned above are also observed. In contrast, sharp resonances are displayed both for aryl- and alkyl- $\text{N}(\text{CH}_3)_2$ groups in the ^1H NMR spectra of complexes **9** and **10**. For complex **9** the resonance of the alkyl- $\text{N}(\text{CH}_3)_2$ group shifts significantly upfield, whereas that of complex **10** shifts slightly downfield. Based on the fact that a significant upfield shift ($\Delta\delta = 0.77\text{--}1$ ppm) of one methyl resonance of alkyl- $\text{N}(\text{CH}_3)_2$ groups is also observed for complexes **4** and **6** that all possess cumyl substituents, the origin of the apparent upfield shift of alkyl- $\text{N}(\text{CH}_3)_2$ resonance observed for complex **9** (cumyl substituted) should be independent of the introduction of the aryl amino group. Variable-temperature ^1H NMR study of complex **10** in toluene- d_8 over the temperature range of 298 to 198 K further witnessed the gradual broadening and splitting into two broad peaks of the sharp alkyl- $\text{N}(\text{CH}_3)_2$ signal with decrease of temperature. Similar behavior was also observed for the aryl- $\text{N}(\text{CH}_3)_2$ signal, which broadened and finally split into two broad peaks at an even lower temperature of 198 K. Although these spectroscopic features could be attributed to the restricted rotation of the methyl groups, based on the quite similar behavior of both amino groups as well as our unpublished work,⁴⁵ a rapid exchange process of these two types of nitrogen donors coordinating to the zinc core alternatively might not be ruled out, which could be frozen out at low temperature on the NMR time scale. Taking the same ligand skeleton into consideration, a similar process might also take place for complex **9**.

Molecular structures of zinc complexes

Single crystals of **1**, **3**, **7**, **9** and **10** suitable for X-ray diffraction studies were obtained by slightly cooling a saturated toluene, n-hexane solution or toluene-pentane mixture respectively. Crystallographic data and results of the refinements are summarized in Table 2, selected bond lengths and angles are listed in Tables 3 and 4. As depicted in Fig. 1, complex **1** has a monomeric structure

Table 1 Selected ^1H NMR data for zinc complexes **1–10** and corresponding ligands

Complex	Ar-OMe/NMe ₂	Alkyl-NMe ₂	Ligand	Ar-OMe/NMe ₂	Alkyl-NMe ₂	Solvent
1	3.11 (s, 3H)	1.93 (br s, 6H)	L¹H	3.37 (s, 3H)	1.93 (s, 6H)	C_6D_6
2	3.10 (s, 3H)	1.92 (br s, 6H)	L²H	3.36 (s, 3H)	1.94 (s, 6H)	C_6D_6
3	3.33 (s, 3H)	2.04 (br s, 3H), 1.74 (br s, 3H)	L³H	3.27 (s, 3H)	1.92 (s, 6H)	C_6D_6
4	3.31 (s, 3H)	1.91 (br s, 3H), 1.14 (br s, 3H)	L⁴H	3.25 (s, 3H)	1.91 (s, 6H)	C_6D_6
5	3.29 (s, 3H)	2.01 (br s, 3H), 1.71 (br s, 3H)	L⁵H	3.27 (s, 3H)	1.82 (s, 6H)	C_6D_6
6	3.78 (s, 3H)	2.02 (br s, 3H), 1.02 (br s, 3H)	L⁶H	3.66 (s, 3H)	2.02 (s, 6H)	CDCl_3
7	3.83 (s, 3H)	2.39 (br s, 3H), 2.15 (br s, 3H)	L⁷H	3.77 (s, 3H)	2.13 (s, 6H)	CDCl_3
8	2.27 (s, 6H)	2.06 (br s, 3H), 1.81 (br s, 3H)	L⁸H	2.38 (s, 6H)	1.94 (s, 6H)	C_6D_6
9	2.54 (s, 6H)	1.49 (s, 6H) ^a	L⁹H	2.53 (s, 6H)	2.03 (s, 6H)	CDCl_3
10	2.60 (s, 6H)	2.26 (s, 6H)	L¹⁰H	2.56 (s, 6H)	2.17 (s, 6H)	CDCl_3

^a This signal is slightly broader than that of complex **10**.

Table 2 Crystallographic data for **1**, **3**, **7**, **9**, **10**

	1	3	7	9	10
Empirical formula	C ₃₀ H ₅₅ N ₅ O ₂ Si ₂ Zn	C ₃₅ H ₆₃ N ₅ O ₂ Si ₂ Zn	C ₃₁ H ₅₈ Cl ₂ N ₂ O ₂ Zn	C ₄₁ H ₅₅ N ₃ OZn	C ₂₃ H ₃₃ Cl ₂ N ₃ OZn
<i>M_r</i>	609.30	679.43	476.72	671.25	503.79
<i>T</i> /K	293(2)	296(2)	296(2)	296(2)	293(2)
Crystal size/mm	0.34 × 0.33 × 0.26	0.25 × 0.20 × 0.20	0.31 × 0.16 × 0.12	0.25 × 0.22 × 0.20	0.42 × 0.37 × 0.21
Crystal system	Orthorhombic	Monoclinic	Monoclinic	Triclinic	Monoclinic
Space group	<i>P</i> 2 ₁ 2 ₁ 2 ₁	<i>P</i> 2 ₁ / <i>c</i>	<i>P</i> 2 ₁ / <i>n</i>	<i>P</i> $\bar{1}$	<i>P</i> 2 ₁ / <i>c</i>
<i>a</i> /Å	12.052(7)	8.9250(10)	10.5566(12)	8.2877(11)	16.3448(17)
<i>b</i> /Å	15.516(9)	24.604(3)	18.482(2)	13.4436(18)	9.4596(10)
<i>c</i> /Å	18.0946(10)	18.129(2)	12.2472(14)	18.389(2)	16.1050(16)
α /°	90	90	90	110.4870(10)	90
β /°	90	95.663(2)	108.060(2)	90.143(2)	97.982(2)
γ /°	90	90	90	100.628(2)	90
<i>V</i> /Å ³	3383.5(3)	3961.4(8)	2271.8(4)	1881.3(4)	2466.0(4)
<i>Z</i>	4	4	4	2	4
<i>D_c</i> /Mg m ⁻³	1.196	1.139	1.394	1.185	1.357
μ /mm ⁻¹	0.825	0.711	1.334	0.686	1.232
<i>F</i> (000)	1312	1472	992	720	1056
θ range/°	1.73–27.00	2.26–25.04	2.07–26.00	2.35–25.05	2.49–25.99
Range <i>hkl</i>	±15, ±19, –17 to 23	–9 to 10, –29 to 18, –20 to 21	±12, –22 to 20, –14 to 15	±9, –13 to 16, –21 to 20	–16 to 20, ±11, ±19
Refins collected/unique	20151/7318	20329/7020	12375/4440	9813/6535	13064/4831
<i>R_{int}</i>	0.0474	0.0564	0.0962	0.0224	0.0940
Max., min. transmission	1.0000, 0.8375	0.8708, 0.8422	1.0000, 0.7298	0.8749, 0.8471	1.0000, 0.7719
Data/restraints/param.	7318/0/356	7020/0/396	4440/0/257	6535/0/425	4831/2/288
Goodness-of-fit on <i>F</i> ²	1.018	1.009	0.856	1.021	0.965
Final <i>R</i> ₁ , <i>wR</i> ₂ [<i>I</i> > 2σ(<i>I</i>)]	0.0412, 0.0811	0.0467, 0.0955	0.0586, 0.0899	0.0435, 0.0933	0.0470, 0.1108
<i>R</i> ₁ , <i>wR</i> ₂ (all data)	0.0463, 0.0829	0.0960, 0.1155	0.1341, 0.1100	0.0607, 0.1027	0.0633, 0.1171
$\Delta\rho_{\max,\min}$ /e Å ⁻³	0.443, –0.274	0.294, –0.285	0.323, –0.403	0.361, –0.318	0.566, –0.331

Table 3 Selected bond lengths (Å) and angles (°) in **1** and **3**

[(L ¹)ZnN(SiMe ₃) ₂] (1)			
Zn–N(3)	1.935(2)	Zn–N(2)	2.150(2)
Zn–O(1)	1.9366(18)	Si(2)–N(3)	1.703(2)
Zn–N(1)	2.1293(19)	Si(1)–N(3)	1.717(2)
Zn...Si(1)	2.979(8)		
N(3)–Zn–O(1)			
O(1)–Zn–N(1)	120.1(9)	N(3)–Zn–N(1)	126.6(9)
O(1)–Zn–N(2)	95.7(7)	N(3)–Zn–N(2)	117.0(9)
C(8)–N(1)–Zn	104.9(9)	N(1)–Zn–N(2)	85.93(8)
C(10)–N(1)–Zn	104.32(14)	C(7)–N(1)–Zn	106.45(15)
C(23)–N(2)–Zn	111.87(14)	C(22)–N(2)–Zn	112.02(18)
Si(2)–N(3)–Si(1)	113.08(18)	C(9)–N(2)–Zn	102.19(15)
Si(1)–N(3)–Zn	122.56(13)	Si(2)–N(3)–Zn	127.18(13)
	109.17(12)	C(1)–O(1)–Zn	126.57(17)
[(L ³)ZnN(SiMe ₃) ₂] (3)			
Zn(1)–N(3)	1.930(3)	Zn(1)–O(1)	1.934(2)
Zn(1)–N(1)	2.136(2)	Zn(1)–N(2)	2.164(3)
Si(1)–N(3)	1.708(3)	Si(2)–N(3)	1.722(3)
Zn...Si(2)	2.986(5)		
N(3)–Zn(1)–O(1)			
O(1)–Zn(1)–N(1)	118.60(11)	N(3)–Zn(1)–N(1)	120.23(12)
O(1)–Zn(1)–N(2)	96.2(9)	N(3)–Zn(1)–N(2)	125.27(12)
C(26)–N(1)–Zn(1)	103.77(11)	N(1)–Zn(1)–N(2)	85.03(10)
C(12)–N(1)–Zn(1)	105.75(19)	C(13)–N(1)–Zn(1)	110.07(18)
C(27)–N(2)–Zn(1)	104.85(18)	C(28)–N(2)–Zn(1)	110.9(2)
Si(1)–N(3)–Si(2)	102.7(2)	C(29)–N(2)–Zn(1)	114.5(2)
Si(2)–N(3)–Zn(1)	121.79(16)	Si(1)–N(3)–Zn(1)	128.41(16)
	109.52(15)	C(1)–O(1)–Zn(1)	127.1(2)

in the solid state in which the zinc atom is four-coordinate by three heteroatom donors of the tetradentate ligand and one bis(trimethylsilyl)amido group adopting a distorted tetrahedral geometry. The coordination of the ether functional group to zinc is not observed in the solid state as evidenced by the long distance

Table 4 Selected bond lengths (Å) and angles (°) in **7**, **9** and **10**

[(L ⁷)ZnEt] (7)			
Zn–O(1)	1.936(3)	Zn–C(20)	1.950(6)
Zn–N(1)	2.156(3)	Zn–N(2)	2.170(4)
O(1)–Zn–C(20)			
C(20)–Zn–N(1)	127.3(2)	O(1)–Zn–N(1)	94.01(13)
C(20)–Zn–N(2)	121.5(2)	O(1)–Zn–N(2)	103.80(16)
C(16)–O(1)–Zn	116.5(3)	N(1)–Zn–N(2)	83.88(15)
C(7)–N(1)–Zn	125.1(3)	C(8)–N(1)–Zn	106.3(3)
C(18)–N(2)–Zn	107.0(3)	C(10)–N(1)–Zn	107.6(3)
C(17)–N(2)–Zn	113.0(3)	C(9)–N(2)–Zn	103.7(3)
	110.4(3)	C(21)–C(20)–Zn	119.9(5)
[(L ⁹)ZnEt] (9)			
Zn(1)–O(1)	1.9205(17)	Zn(1)–C(1)	1.966(3)
Zn(1)–N(1)	2.158(2)	Zn(1)–N(2)	2.176(2)
O(1)–Zn(1)–C(1)			
C(1)–Zn(1)–N(1)	120.79(11)	O(1)–Zn(1)–N(1)	94.18(7)
C(1)–Zn(1)–N(2)	123.81(11)	O(1)–Zn(1)–N(2)	107.09(8)
C(2)–C(1)–Zn(1)	119.60(12)	N(1)–Zn(1)–N(2)	83.46(8)
C(17)–N(1)–Zn(1)	113.2(3)	C(3)–N(1)–Zn(1)	105.75(15)
C(5)–N(2)–Zn(1)	107.73(15)	C(7)–N(1)–Zn(1)	104.80(14)
C(6)–N(2)–Zn(1)	108.97(17)	C(4)–N(2)–Zn(1)	105.36(16)
	113.57(19)	C(23)–O(1)–Zn(1)	129.95(16)
[(L ¹⁰)ZnEt] (10)			
Zn–O(1)	1.952(2)	Zn–C(20)	1.954(4)
Zn–N(1)	2.150(2)	Zn–N(2)	2.162(3)
O(1)–Zn–C(20)			
C(20)–Zn–N(1)	122.58(17)	O(1)–Zn–N(1)	94.1(9)
C(20)–Zn–N(2)	123.57(14)	O(1)–Zn–N(2)	105.4(10)
C(16)–O(1)–Zn	119.28(16)	N(1)–Zn–N(2)	83.3(9)
C(8)–N(1)–Zn	124.26(19)	C(10)–N(1)–Zn	107.15(17)
C(18)–N(2)–Zn	107.17(16)	C(7)–N(1)–Zn	104.99(16)
C(17)–N(2)–Zn	112.1(2)	C(9)–N(2)–Zn	104.43(17)
C(21)–C(20)–Zn	110.4(2)	C(21)–C(20)–Zn	115.0(12)
	126.4(6)		

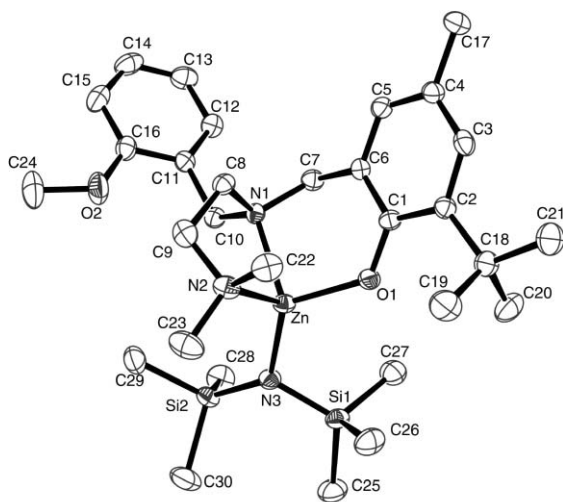


Fig. 1 ORTEP diagram of the molecular structure of $[(L^1)ZnN(SiMe_3)_2]$ (**1**). Thermal ellipsoids are drawn at the 30% probability level. Hydrogen atoms are omitted for clarity.

of $Zn \cdots O2$ (4.867(2) Å). The bond length of the zinc to silylamido nitrogen atom ($Zn-N3$) in complex **1** is 1.935(2) Å, which is slightly longer than those in β -diketiminato zinc silylamido complexes (1.881–1.896 Å).^{37,46,47} The bond distances of $Zn-N1$ and $Zn-N2$ are 2.1293(19) and 2.150(2) Å respectively, fall into the range of $Zn-N$ coordinated bond lengths in common zinc complexes (2.058–2.324 Å).^{33,39,48–50} Being attributed to the steric repulsion between the ligand and the silylamido group, the angles of $N3-Zn-N2 = 117.00(9)^\circ$, $N3-Zn-N1 = 126.61(9)^\circ$ and $O1-Zn-N3 = 120.05(9)^\circ$ deviate significantly from the normal value of 109.47° . The molecular structure of complex **3** (Fig. 2) is similar to that described for complex **1**, except that, in complex **3** the methoxy group on the phenyl moiety and the $NCH_2CH_2N(CH_3)_2$ bridge are “*trans*” oriented with respect to the plane constructed by $Zn1$, $N1$, $C13$ atoms, whereas those in **1** are in “*syn*” form, which is also clear when we look at the corresponding angles of $N2-$

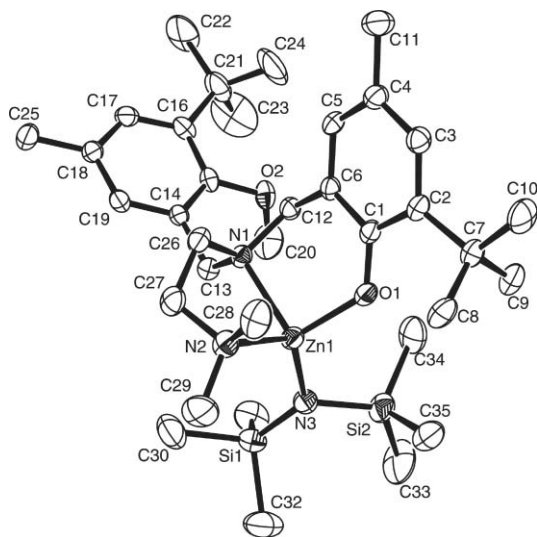


Fig. 2 ORTEP diagram of the molecular structure of $[(L^3)ZnN(SiMe_3)_2]$ (**3**). Thermal ellipsoids are drawn at the 30% probability level. Hydrogen atoms are omitted for clarity.

$Zn-O2$ (122.33° in **3** vs. 67.36° in **1**). In addition, the angle of $N3-Zn-N1 = 126.61(9)^\circ$ in complex **3** is significantly more open than that in complex **1** ($120.23(12)^\circ$), whereas the angle of $N3-Zn-N2 = 117.00(9)^\circ$ is much smaller than that in complex **1** ($125.27(15)^\circ$). All these mentioned features are obviously related with the introduction of the second steric demanding *tert*-butyl group, which causes reasonable changes of the coordination parameters of the ligand wrapping around the zinc center.

Similar to zinc silylamido complexes **1** and **3**, the oxygen atom of the ether functional group in complex **7** is not coordinate to zinc core as indicated by the corresponding distance of $Zn \cdots O2 = 4.995(4)$ Å (Fig. 3). The coordination of the nitrogen atom of the $N(CH_3)_2$ functional group on phenyl to zinc atom is not observed either in the solid state structures of complexes **9** and **10** ($Zn \cdots N3$ distances are 4.8697(30) and 5.196(4) Å, respectively) (Figs 4 and 5). All these donor groups adopt “*syn*” orientation towards the $NCH_2CH_2N(CH_3)_2$ bridge with respect to the $Zn1-N1-C13$ plane, indicating a less hindered environment in complexes **7**, **9**, **10** in comparison with that in complex **3**. Although bearing the same chloro substituents at the *ortho*- and *para*-positions of the phenoxide group, complex **7** possesses different coordination

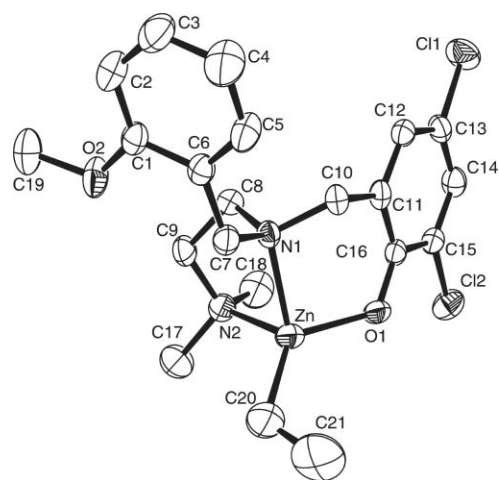


Fig. 3 ORTEP diagram of the molecular structure of $[(L^7)ZnEt]$ (**7**). Thermal ellipsoids are drawn at the 30% probability level. Hydrogen atoms are omitted for clarity.

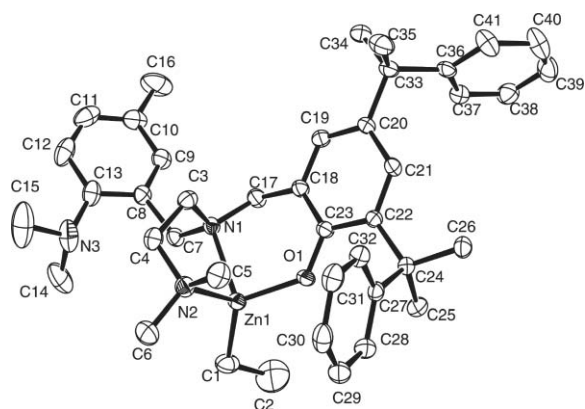


Fig. 4 ORTEP diagram of the molecular structure of $[(L^9)ZnEt]$ (**9**). Thermal ellipsoids are drawn at the 30% probability level. Hydrogen atoms are omitted for clarity.

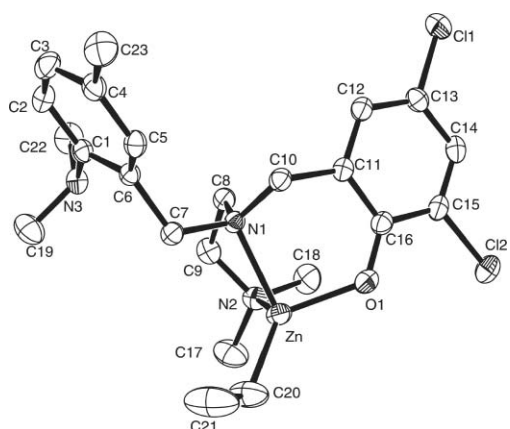


Fig. 5 ORTEP diagram of the molecular structure of $[(L^{10})ZnEt]$ (**10**). Thermal ellipsoids are drawn at the 30% probability level. Hydrogen atoms are omitted for clarity.

parameters from those of complex **10**, which are however more similar to those of complex **9**. In complex **7**, the angle of C20–Zn–O1 ($127.3(2)^\circ$) is significantly larger than those in the other zinc complexes of this work ($118.60(11)^\circ$ – $122.58(17)^\circ$), while the angles of C20–Zn–N1 ($121.5(2)^\circ$) and C20–Zn–N2 ($116.5(3)^\circ$) are

slightly smaller. The other structural features of complexes **7**, **9**, **10** are however similar.

Ring-opening polymerization of *rac*-lactide

As can be seen from the data compiled in Table 5, the zinc silylamido complexes **1–5** and **8** are active initiators for the ring-opening polymerization of *rac*-lactide at ambient temperature in THF or toluene. In each case, high conversion of monomer to PLA could be achieved within 50 min (74–95%). The polymers produced in either solvent have high molecular weights and relatively broad molecular weight distributions ($M_w/M_n = 1.51$ – 1.93). The molecular weights of polymer samples obtained in THF are close to the theoretical values, whereas those obtained in toluene deviate from the calculated values significantly.

The structure of the ancillary ligands also has considerable influence on the catalytic activity. It is found that the presence of substituents, particularly, at *ortho*-position of the phenoxide unit of the ligand, plays an important role in determining the polymerization rate. In general, the introduction of bulky substituents leads to a decrease of the polymerization rate. Complex **4** with both bulky cumyl and *tert*-butyl groups exhibits the lowest catalytic activity for the polymerization of *rac*-lactide among complexes **1–5** and **8**. Although being far away from the metal center evidenced by the results of X-ray diffraction

Table 5 Ring-opening polymerization of *rac*-lactide initiated by zinc silylamido complexes **1–5** and **8**^a

Run	Cat.	$[LA]_0/[Zn]_0/[iPrOH]_0$	Solvent	$T/^\circ C$	t/min	Conv. ^b (%)	$10^{-4}M_{n,\text{calc}}^c$	$10^{-4}M_n^d$	M_w/M_n^d	P_m^e
1	1	200:1:0	THF	25	40	95	2.72	4.14	1.51	0.51
2		200:1:1	THF	25	4	84	2.42		0.48	
3		200:1:1	THF	25	9	92	2.66	2.69	1.48	0.48
4		200:1:0	Tol	24	50	87	2.50	4.03	1.86	0.45
5		200:1:1	Tol	25	5	77	2.22	1.89	1.53	0.43
6		200:1:1	Tol	25	9	98	2.84			0.43
7	2	200:1:0	THF	25	40	97	2.79	2.61	1.53	0.50
8		200:1:1	THF	25	4	98	2.82	2.48	1.40	0.49
9		200:1:0	Tol	25	50	98	2.81	2.18	1.86	0.46
10		200:1:1	Tol	25	5	98	2.84	1.98	1.44	0.44
11	3	200:1:0	THF	26	50	89	2.57	2.97	1.93	0.52
12		200:1:1	THF	25	9	90	2.60	2.73	1.10	0.45
13		200:1:0	Tol	24	50	84	2.43	4.16	1.47	0.48
14		200:1:1	Tol	24	9	91	2.64	1.43	1.16	0.42
15	4	200:1:0	THF	24	50	85	2.46	2.34	1.76	0.60
16		200:1:0	THF	–40	1020	10	0.29			0.54
17		200:1:1	THF	25	10	80	2.31	1.00	1.24	0.54
18		200:1:0	Tol	25	50	74	2.13	4.17	1.59	0.57
19		200:1:1	Tol	25	9	91	2.63	1.60	1.17	0.49
20		2000:1:5	Tol	25	60	71	4.08	2.31	1.09	0.50
21	5	200:1:0	THF	24	15	67	1.94	2.87	1.71	0.41
22		200:1:1	THF	24	5	95	2.73	2.61	1.22	0.37
23		200:1:0	Tol	25	30	92	2.66	6.42	1.57	0.33
24		200:1:1	Tol	25	4	95	2.74	2.09	1.45	0.35
25	8	200:1:0	THF	24	40	95	2.75	2.81	1.44	0.51
26		200:1:1	THF	24	4	97	2.80	1.96	1.29	0.46
27		200:1:0	Tol	25	50	84	2.42	3.18	1.53	0.48
28		200:1:1	Tol	25	5	98	2.83	1.49	1.34	0.44

^a $[rac-LA]_0 = 1.0$ M. ^b Determined by 1H NMR spectroscopy. ^c $M_{n,\text{calc}} = ([LA]_0/[Zn]_0) \times 144.13 \times \text{conv.}$; with the presence of $iPrOH$, $M_{n,\text{calc}} = ([LA]_0/[iPrOH]_0) \times 144.13 \times \text{conv.} + 60$. ^d Determined by GPC. ^e P_m is the probability of forming a new *m*-dyad, determined by homonuclear decoupled 1H NMR spectroscopy.

studies, the substituents on the phenyl ether moiety influence the activity as well when comparing the polymerization runs initiated by complexes **1** and **3**. It is easy to understand that the presence of bulky groups in the coordination sphere of the central metal tends to block the coordination/insertion of incoming monomer and hence is disadvantageous to the catalytic activity. The introduction of chloro groups to phenoxide unit of the ligand in complex **5** has a different effect; on one hand the less-hindered chloro substituents would make the zinc core more accessible for the incoming monomer, on the other hand the electron withdrawing effect of chloro groups would enhance greatly the electrophilicity of the zinc center. The increase of activity of complex **5** towards lactide polymerization should be a combined consequence of both aspects. A similar phenomenon was observed by Gibson *et al.* in the polymerization of *rac*-lactide with an aluminium complex supported by a tetradentate aminophenoxide ligand, which involved four chloro substituents at the *ortho*- and *para*-positions of phenoxide units.⁵¹ Nevertheless, there was an opposite trend for lactide polymerization with zinc³⁹ and magnesium⁵² complexes supported by NNO-tridentate Schiff-base ligands which only possessed halo substituent at the *para*-position of the phenoxide.

Upon addition of isopropanol, the activities of zinc amide complexes **1–5** and **8** increase significantly, high conversion of monomer to PLA up to 98% could be reached just within minutes when a molar ratio of $[LA]_0/[Zn]_0 = 200$ was adopted. Even for 2000 equiv. of *rac*-lactide, in the presence of 5 equiv. of isopropanol the polymerization initiated by complex **4** still proceeded smoothly to 71% in 1 h (run 20) and produced poly(lactides) with an average number molecular weight of $2.31 \times 10^4 \text{ g mol}^{-1}$ and a narrow PDI value of 1.09. To acquire some information about ROP of lactide initiated by *in situ* generated zinc isopropoxide, NMR-scale polymerization was conducted with $[rac-LA]_0 : [Zn]_0 : [iPrOH]_0 = 20 : 1 : 1$, the polymerization started instantaneously and active oligomer could be identified unambiguously (Fig. 6).⁵³ The addition of a second equiv. of isopropanol did not decompose the active oligomer, the polymerization rate was increased instead, giving rise to an “immortal” ROP of *rac*-lactide. The ¹H NMR spectra of the isolated poly(lactides) showed that the polymer chains are end-capped by isopropyl ester and hydroxyl groups, indicating a coordination-insertion mechanism.

Zinc ethyl complexes **6**, **7**, **9**, **10** can not initiate the polymerization of *rac*-lactide at ambient or elevated temperature through ethyl initiation. In the presence of added isopropanol, desirable polymerization results could be achieved at 60 °C (Table 6), and

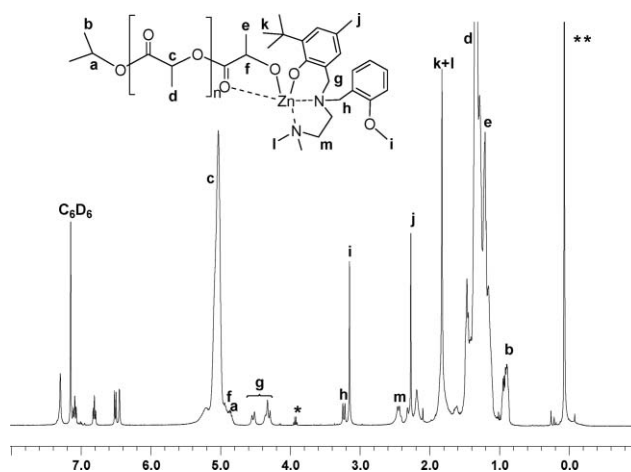


Fig. 6 ¹H NMR spectrum (400 MHz, C₆D₆) of active *rac*-lactide oligomer by **1**/*i*PrOH (*, monomer; **, free HN(SiMe₃)₂); $[LA]_0 : [Zn]_0 : [iPrOH]_0 = 20 : 1 : 1$, at 20 °C.

gave PLAs with narrow molecular weight distributions ($M_w/M_n = 1.08–1.20$). However, the molecular weights of the obtained polymer samples are much lower than the theoretical values. To gain some insights into the structure of the assumed zinc isopropoxide initiator, the reaction of zinc ethyl complex **9** with one equiv. of isopropanol was monitored by ¹H NMR spectroscopy. The alcoholysis reaction occurred only at relatively high temperature and unexpectedly proved to be quite slow; full conversion could not be reached even after 8 h at 60 °C. Thus it is conceivable that under polymerization conditions such reaction might be accelerated to a certain degree in the presence of monomer, but still could not reach full conversion; the residual isopropanol then acted as a chain transfer agent and led to the decrease of molecular weights. From the ratios of measured molecular weights and the calculated ones (Table 6), around 40–65% of zinc ethyl complexes were estimated to be converted to the active metal alkoxide initiators. Furthermore, in the presence of isopropanol, complexes **7** and **10** with 4,6-dichloro-substitution exhibit higher catalytic activities than complexes **6** and **9** with bulky cumyl substituents. Complexes **9** and **10** possess a dimethylamino donor on one of the phenyl rings in the ligand framework instead a methoxy group, which do have some influence on the activity. In either THF or toluene complexes **9** and **10** show higher activities than their methoxy analogues, for which we do not have reasonable explanation yet.

Table 6 Ring-opening polymerization of *rac*-lactide initiated by zinc ethyl complexes **6**, **7**, **9**, **10** in the presence of isopropanol^a

Run	Cat.	$[LA]_0/[Zn]_0/[iPrOH]_0$	Solvent	$T/^\circ\text{C}$	t/min	Conv. ^b (%)	$10^{-4}M_{n,\text{calcd}}^c$	$10^{-4}M_n^d$	M_w/M_n^d	P_m^e
1	6	200 : 1 : 1	THF	60	240	55	1.60	1.02	1.08	0.53
2		200 : 1 : 1	Tol	60	100	74	2.13	1.09	1.08	0.53
3	7	200 : 1 : 1	THF	60	250	76	2.20	1.21	1.07	0.44
4		200 : 1 : 1	Tol	60	60	72	2.07	1.04	1.09	0.42
5	9	200 : 1 : 1	THF	60	240	62	1.78	0.53	1.17	0.54
6		200 : 1 : 1	Tol	60	100	79	2.27	0.84	1.12	0.54
7	10	200 : 1 : 1	THF	60	250	83	2.41	1.17	1.20	0.44
8		200 : 1 : 1	Tol	60	60	78	2.25	1.39	1.09	0.43

^a $[rac-LA]_0 = 1.0 \text{ M}$, $[Zn]_0 = 0.005 \text{ M}$. ^b Determined by ¹H NMR spectroscopy. ^c $M_{n,\text{calcd}} = ([LA]_0/[iPrOH]_0) \times 144.13 \times \text{conv.} + 60$. ^d Determined by GPC. ^e P_m is the probability of forming a new *m*-dyad, determined by homonuclear decoupled ¹H NMR spectroscopy.

Microstructure analyses of PLAs were achieved through inspecting the methine region of homonuclear decoupled ^1H NMR spectra of the resultant polymers. Complex **4** with sterically demanding cumyl groups at the *ortho*- and *para*-positions of phenoxide unit shows certain preference for isotactic dyad enchainment during lactide polymerization ($P_m = 0.60$, in THF), whereas complex **5** with less hindered chloro-substituent displays certain preference for heterotactic dyad enchainment ($P_r = 0.67$, in toluene). Gibson *et al.*⁵¹ found that for aluminium complexes with Salan-type bis(phenolato) ligands, the replacement of hydrogen atom at the *ortho*-position of phenoxide with a methyl led to a dramatic decrease of P_m value from 0.79 to 0.19. An isotactic dyad preference in *rac*-lactide polymerization was achieved with Group 4 complexes bearing the same type of bis(phenolato) ligand with smaller *ortho*-methyl group instead of those with bulky *ortho*-group.⁵⁴ Concerning this inconsistency, we think that it may relate with the structure of the real active species. It is generally accepted that for lactide polymerization, regardless of the type of initiation groups, upon coordination and insertion of the first monomer, metal alkoxide species are formed, which are known to aggregate easily in solution.³⁶ The presence of sterically demanding groups in the vicinity of donor atoms such as phenoxide oxygen atom might be likely to prevent such aggregation. Thus the assumed asymmetric monomeric metal center might plausibly induce isotactic selectivity for *rac*-lactide polymerization to a certain degree depending on the stability of chiral environment around the metal (the fluxionality of the ligand framework). The aggregation of formed metal alkoxides might not be avoided in complex **5** due to the less hindered chloro substituents, and may enable a chain-end control to afford heterotactic-enriched PLA.

Conclusions

In conclusion, several monomeric zinc silylamido and ethyl complexes **1–10** supported by non-symmetric tetradentate aminophenolate ligands were synthesized and structurally characterized. X-Ray diffraction studies reveal that all the complexes possess a four-coordinate zinc center. The substituent CH_3O or $\text{N}(\text{CH}_3)_2$ on one phenyl moiety is not coordinated to the zinc center in the solid state; only the other three heteroatom donors of the tetradentate ligand and bis(trimethylsilyl)amido or ethyl group chelate to zinc atom adopting a distorted tetrahedral geometry. The zinc silylamido complexes **1–5** and **8** acted as highly active single-component initiators for the ring-opening polymerization of *rac*-lactide at room temperature in THF or toluene, providing polymers with a certain degree of tacticity. Addition of isopropanol may significantly raise the polymerization rate. Zinc ethyl complexes **7**, **9** and **10** could not initiate the ring-opening polymerization of *rac*-lactide; zinc isopropoxides formed by *in situ* alcoholysis of the ethyl complexes successfully initiated the polymerization of *rac*-lactide at 60 °C in THF or toluene and afforded the PLAs with narrow molecular weight distributions. The activity and selectivity in the polymerization of *rac*-lactide using complexes **1–10** as initiators/catalysts depend upon the ligand substitution pattern to a certain extent. The introduction of steric bulky substituents increases the amount of isotactic dyad along the growing polymer chain and reduces the polymerization rate. Notably, electron-withdrawing substituents

dramatically raise the activity in the polymerization process and favor the heterotactic dyad enchainment.

Experimental

General considerations

All manipulations were carried out under a dry argon atmosphere using standard Schlenk-line or glove-box techniques. Toluene and n-hexane were refluxed over sodium benzophenone ketyl prior to use. Benzene- d_6 , toluene- d_8 , chloroform- d and other reagents were carefully dried and stored in a glove-box. $[\text{ZnN}(\text{SiMe}_3)_2]$ was synthesized according to the literature method.⁵⁵ 3-*tert*-Butyl-5-methyl-2-methoxybenzaldehyde,^{56,57} 2-(*N,N*-dimethyl)amino-5-methylbenzaldehyde,⁵⁸ were prepared according to the reported methods. *rac*-Lactide (Aldrich) was recrystallized with dry toluene and then sublimed twice under vacuum at 80 °C. 2-Propanol was dried over calcium hydride prior to distillation. All other chemicals were commercially available and used after appropriate purification. Glassware and vials used in the polymerization were dried in an oven at 120 °C overnight and exposed to vacuum-argon cycle three times.

NMR spectra were recorded on Bruker AVANCE-400 and Bruker AVANCE-500 spectrometers at 25 °C (^1H : 400, 500 MHz; ^{13}C : 100 MHz) unless otherwise stated. Chemical shifts for ^1H and ^{13}C NMR spectra were referenced internally using the residual solvent resonances and reported relative to tetramethylsilane (TMS). Elemental analyses were performed on an EA-1106 instrument. Spectroscopic analyses of polymers were performed in CDCl_3 . Gel permeation chromatography (GPC) analyses were carried out on a Waters instrument (M1515 pump, Optilab Rex injector) in THF at 25 °C, at a flow rate of 1 mL min^{-1} . Calibration standards were commercially available narrowly distributed linear polystyrene samples that cover a broad range of molar masses ($10^3 < M < 2 \times 10^6 \text{ g mol}^{-1}$).

Syntheses

6-*tert*-Butyl-2- $\{N$ -(2-methoxybenzyl)- N -[2-(*N,N*-dimethyl)aminoethyl]aminomethyl}-4-methylphenol (L'H). *N,N*-Dimethylethylenediamine (2.64 g, 30.0 mmol) and a solution of 2-methoxybenzaldehyde (4.08 g, 30.0 mmol) in methanol (20 mL) were heated to reflux for 24 h. After cooling to r.t., sodium borohydride (2.28 g, 60.0 mmol) was sequentially added to the above yellow solution at 0 °C (ice-water bath) and the mixture was stirred for 12 h. The reaction mixture was extracted with methylene dichloride. The organic phase was dried over anhydrous MgSO_4 . Removal of the solvent by rotary evaporation gave a viscous oil, to which was added a solution of paraformaldehyde (0.900 g, 30.0 mmol) and 2-*tert*-butyl-4-methylphenol (4.92 g, 30.0 mmol) in methanol (20 mL) at 80 °C during 12 h with magnetic stirring. The mixture was cooled and concentrated under vacuum to give an oil, which was purified by column chromatography (silica gel 100 Merck, light petroleum–ethyl acetate 10:1) to provide white solids after removal of all the volatiles (4.93 g, 42.8%). Anal. Calc. for $\text{C}_{24}\text{H}_{36}\text{N}_2\text{O}_2$: C, 74.96; H, 9.44; N, 7.28. Found: C, 75.22; H, 9.54; N, 7.25%. ^1H NMR (CDCl_3 , 400 MHz): δ 10.75 (s, 1H, OH), 7.28–7.23 (m, 2H, ArH), 6.97 (d, 1H, $^4J = 1.8 \text{ Hz}$, ArH), 6.92 (td, 1H, $^3J = 8.0 \text{ Hz}$, $^4J = 1.0 \text{ Hz}$, ArH), 6.88

(dd, 1H, $^3J = 8.0$ Hz, $^4J = 1.0$ Hz, ArH), 6.68 (d, 1H, $^4J = 1.8$ Hz, ArH), 3.86 (s, 3H, CH₃O-Ar), 3.74 (s, 2H, Ar-CH₂-N), 3.72 (s, 2H, N-CH₂-Ar), 2.61 (d, 1H, $^3J = 6.6$ Hz, CH₂CH₂), 2.59 (d, 1H, $^3J = 5.5$ Hz, CH₂CH₂), 2.44 (d, 1H, $^3J = 6.6$ Hz, CH₂CH₂), 2.42 (d, 1H, $^3J = 5.5$ Hz, CH₂CH₂), 2.24 (s, 3H, Ar-CH₃), 2.12 (s, 6H, N(CH₃)₂), 1.43 (s, 9H, C(CH₃)₃). ¹H NMR (C₆D₆, 400 MHz): δ 10.90 (s, 1H, OH), 7.33 (d, 1H, $^3J = 7.7$ Hz, ArH), 7.17 (s, 1H, ArH), 7.05 (t, 1H, $^3J = 7.7$ Hz, ArH), 6.85 (t, 1H, $^3J = 7.7$ Hz, ArH), 6.67 (s, 1H, ArH), 6.51 (d, 1H, $^3J = 7.7$ Hz, ArH), 3.68 (s, 2H, Ar-CH₂-N), 3.58 (s, 2H, N-CH₂-Ar), 3.37 (s, 3H, CH₃O-Ar), 2.49 (t, 2H, $^3J = 6.5$ Hz, CH₂CH₂), 2.24 (t, 2H, $^3J = 6.5$ Hz, CH₂CH₂), 2.24 (s, 3H, Ar-CH₃, overlapped with CH₂CH₂), 1.93 (s, 6H, N(CH₃)₂), 1.67 (s, 9H, C(CH₃)₃). ¹³C{¹H} NMR (CDCl₃, 100 MHz): δ 158.0, 154.4, 136.1, 131.4, 128.7, 127.5, 126.6, 126.3, 125.6, 122.6, 120.3, 110.3 (all Ar-C), 58.2 (CH₃O-Ar), 56.6 (Ar-CH₂-N), 55.1 (N-CH₂-Ar), 53.1 (CH₂CH₂), 50.6 (CH₂CH₂), 45.6 (N(CH₃)₂), 34.5 (C(CH₃)₃), 29.5 (C(CH₃)₃), 20.8 (Ar-CH₃).

4,6-Di-*tert*-butyl-2-*N*-(2-methoxybenzyl)-*N*-[2-(*N,N*-dimethylaminoethyl)aminomethyl]phenol (L²H). The procedure was same as that of L¹H, except that 2,4-di-*tert*-butylphenol (6.18 g, 30.0 mmol) were used to afford ligand L²H as a viscous oil (5.28 g, 41.3%). Anal. Calc. for C₂₇H₄₂N₂O₂: C, 76.01; H, 9.92; N, 6.57. Found: C, 75.97; H, 9.88; N, 6.48%. ¹H NMR (CDCl₃, 400 MHz): δ 10.82 (s, 1H, OH), 7.25 (d, 1H, $^3J = 7.8$ Hz, ArH, overlapped by C₆D₆ signal), 7.24 (t, 1H, $^3J = 7.8$ Hz, ArH), 7.17 (d, 1H, $^4J = 2.2$ Hz, ArH), 6.9 (t, 1H, $^3J = 7.8$ Hz, ArH), 6.87 (d, 1H, $^3J = 7.8$ Hz, ArH), 6.83 (d, 1H, $^4J = 2.2$ Hz, ArH), 3.86 (s, 3H, CH₃O-Ar), 3.75 (s, 2H, Ar-CH₂-N), 3.74 (s, 2H, N-CH₂-Ar), 2.60 (d, 1H, $^3J = 6.6$ Hz, CH₂CH₂), 2.58 (d, 1H, $^3J = 7.2$ Hz, CH₂CH₂), 2.43 (d, 1H, $^3J = 6.6$ Hz, CH₂CH₂), 2.42 (d, 1H, $^3J = 7.2$ Hz, CH₂CH₂), 2.11 (s, 6H, N(CH₃)₂), 1.42 (s, 9H, C(CH₃)₃), 1.27 (s, 9H, C(CH₃)₃). ¹H NMR (C₆D₆, 400 MHz): δ 11.04 (s, 1H, OH), 7.48 (d, 1H, $^4J = 2.3$ Hz, ArH), 7.34 (dd, 1H, $^4J = 1.4$ Hz, $^3J = 7.4$ Hz, ArH), 7.05 (td, 1H, $^4J = 1.4$ Hz, $^3J = 7.4$ Hz, ArH), 6.97 (d, 1H, $^4J = 2.3$ Hz, ArH), 6.84 (td, 1H, $^4J = 1.4$ Hz, $^3J = 7.4$ Hz, ArH), 6.50 (d, 1H, $^3J = 7.4$ Hz, ArH), 3.70 (s, 2H, Ar-CH₂-N), 3.62 (s, 2H, N-CH₂-Ar), 3.36 (s, 3H, CH₃O-Ar), 2.50 (t, 2H, $^3J = 6.6$ Hz, CH₂CH₂), 2.25 (t, 2H, $^3J = 6.6$ Hz, CH₂CH₂), 1.94 (s, 6H, N(CH₃)₂), 1.71 (s, 9H, C(CH₃)₃), 1.36 (s, 9H, C(CH₃)₃). ¹³C{¹H} NMR (CDCl₃, 100 MHz): δ 158.1, 154.2, 140.0, 135.4, 131.4, 128.7, 125.7, 123.6, 122.5, 121.8, 120.3, 110.3 (all Ar-C), 58.5 (CH₃O-Ar), 56.6 (Ar-CH₂-N), 55.1 (N-CH₂-Ar), 53.1 (CH₂CH₂), 50.6 (CH₂CH₂), 45.5 (N(CH₃)₂), 34.8 (C(CH₃)₃), 34.0 (C(CH₃)₃), 31.7 (C(CH₃)₃), 29.6 (C(CH₃)₃).

6-*tert*-Butyl-2-*N*-(3-*tert*-butyl-2-methoxy-5-methylbenzyl)-*N*-[2-(*N,N*-dimethylaminoethyl)aminomethyl]-4-methylphenol (L³H). *N,N*-Dimethylethylenediamine (2.64 g, 30.0 mmol) and a solution of 3-*tert*-butyl-5-methyl-2-methoxybenzaldehyde (6.18 g, 30.0 mmol) in methanol (20 mL) were heated to reflux for 24 h. After cooling to r.t., sodium borohydride (2.28 g, 60.0 mmol) was sequentially added to the above yellow solution at 0 °C (ice-water bath). After 12 h, the reaction mixture was extracted to give a viscous oil, to which was added a solution of paraformaldehyde (0.900 g, 30.0 mmol) and 2-*tert*-butyl-4-methylphenol (4.92 g, 30.0 mmol) in methanol (20 mL) at 80 °C during 12 h and give an oil, which was purified by column chromatography (silica gel 100 Merck, light petroleum-ethyl acetate 10 : 1) to provide white

solids (7.22 g, 53.0%). Anal. Calc. for C₂₉H₄₆N₂O₂: C, 76.65; H, 10.13; N, 6.17. Found: C, 76.61; H, 10.30; N, 6.04%. ¹H NMR (CDCl₃, 400 MHz): δ 10.62 (s, 1H, OH), 7.07 (d, 1H, $^4J = 1.8$ Hz, ArH), 7.00 (d, 1H, $^4J = 2.2$ Hz, ArH), 6.99 (d, 1H, $^4J = 2.2$ Hz, ArH), 6.73 (d, 1H, $^4J = 1.8$ Hz, ArH), 3.69 (s, 2H, Ar-CH₂-N), 3.64 (s, 3H, CH₃O-Ar), 3.62 (s, 2H, N-CH₂-Ar), 2.54 (d, 1H, $^3J = 6.1$ Hz, CH₂CH₂), 2.53 (d, 1H, $^3J = 6.6$ Hz, CH₂CH₂), 2.45 (d, 1H, $^3J = 6.6$ Hz, CH₂CH₂), 2.45 (d, 1H, $^3J = 6.1$ Hz, CH₂CH₂), 2.261 (s, 3H, Ar-CH₃), 2.257 (s, 3H, Ar-CH₃), 2.13 (s, 6H, N(CH₃)₂), 1.47 (s, 9H, C(CH₃)₃), 1.38 (s, 9H, C(CH₃)₃). ¹H NMR (C₆D₆, 400 MHz): δ 10.69 (s, 1H, OH), 7.29 (d, 1H, $^4J = 1.9$ Hz, ArH), 7.23 (d, 1H, $^4J = 1.9$ Hz, ArH), 7.04 (d, 1H, $^4J = 1.9$ Hz, ArH), 6.78 (d, 1H, $^4J = 1.9$ Hz, ArH), 3.58 (s, 2H, Ar-CH₂-N), 3.51 (s, 2H, N-CH₂-Ar), 3.27 (s, 3H, CH₃O-Ar), 3.36 (t, 2H, $^3J = 6.2$ Hz, CH₂CH₂), 2.29 (s, 3H, Ar-CH₃), 2.25 (s, 3H, Ar-CH₃), 2.13 (t, 2H, $^3J = 6.2$ Hz, CH₂CH₂), 1.92 (s, 6H, N(CH₃)₂), 1.72 (s, 9H, C(CH₃)₃), 1.42 (s, 9H, C(CH₃)₃). ¹³C{¹H} NMR (CDCl₃, 100 MHz): δ 156.7, 154.2, 142.1, 136.4, 132.5, 131.4, 130.1, 128.1, 126.9, 126.6, 123.1 (all Ar-C), 62.5 (CH₃O-Ar), 57.6 (Ar-CH₂-N), 56.3 (N-CH₂-Ar), 52.6 (CH₂CH₂), 50.6 (CH₂CH₂), 45.2 (N(CH₃)₂), 34.9 (C(CH₃)₃), 34.7 (C(CH₃)₃), 31.1 (C(CH₃)₃), 29.6 (C(CH₃)₃), 21.0 (Ar-CH₃), 20.8 (Ar-CH₃).

2-*N*-(3-*tert*-Butyl-2-methoxy-5-methylbenzyl)-*N*-[2-(*N,N*-dimethylaminoethyl)aminomethyl]-4,6-dicumylphenol (L⁴H). *N,N*-Dimethylethylenediamine (2.64 g, 30.0 mmol) and a solution of 3-*tert*-butyl-5-methyl-2-methoxybenzaldehyde (6.18 g, 30.0 mmol) in methanol (20 mL) were heated to reflux for 24 h. After cooling, sodium borohydride (2.28 g, 60.0 mmol) was sequentially added to the above yellow solution at 0 °C and the mixture was stirred for 12 h. The reaction mixture was extracted to give a viscous oil, to which was added a solution of paraformaldehyde (0.900 g, 30.0 mmol) and 2, 4-dicumylphenol (9.90 g, 30.0 mmol) in methanol (20 mL) at 80 °C during 12 h to give an oil, which was purified by column chromatography (silica gel 100 Merck, light petroleum-ethyl acetate 10 : 1) to provide colorless crystals (9.29 g, 48.7%). Anal. Calc. for C₄₂H₅₆N₂O₂: C, 81.24; H, 9.09; N, 4.51. Found: C, 81.02; H, 9.49; N, 4.24%. ¹H NMR (CDCl₃, 400 MHz): δ 10.42 (s, 1H, OH), 7.25–7.13 (m, 10H, ArH), 7.09 (tt, 1H, $^3J = 6.7$ Hz, $^4J = 1.7$ Hz, ArH), 6.97 (d, 1H, $^4J = 1.7$ Hz, ArH), 6.80 (d, 1H, $^4J = 1.7$ Hz, ArH), 6.77 (d, 1H, $^4J = 2.2$ Hz, ArH), 3.56 (s, 5H, CH₃O-Ar, overlapped with Ar-CH₂-N), 3.52 (s, 2H, N-CH₂-Ar), 2.38 (d, 1H, $^3J = 6.4$ Hz, CH₂CH₂), 2.37 (d, 1H, $^3J = 7.3$ Hz, CH₂CH₂), 2.27 (d, 1H, $^3J = 6.4$ Hz, CH₂CH₂), 2.26 (d, 1H, $^3J = 7.3$ Hz, CH₂CH₂), 2.19 (s, 3H, Ar-CH₃), 1.99 (s, 6H, N(CH₃)₂), 1.70 (s, 6H, CMe₂Ph), 1.68 (s, 6H, CMe₂Ph), 1.35 (s, 9H, C(CH₃)₃). ¹H NMR (C₆D₆, 400 MHz): δ 10.69 (s, 1H, OH), δ 7.56 (d, 1H, $^4J = 2.4$ Hz, ArH), 7.46 (dd, 2H, $^3J = 8.2$ Hz, $^4J = 1.2$ Hz, ArH), 7.36 (dd, 2H, $^3J = 8.2$ Hz, $J = 1.0$ Hz, CMe₂Ph), 7.21–7.01 (m, 8H, ArH and CMe₂Ph), 6.91 (d, 1H, $^4J = 2.4$ Hz, ArH), 3.49 (s, 2H, Ar-CH₂-N), 3.27 (s, 2H, N-CH₂-Ar), 3.25 (s, 3H, CH₃O-Ar), 2.19 (s, 3H, Ar-CH₃), 2.18 (t, 2H, $^3J = 6.2$ Hz, CH₂CH₂), 1.95 (t, 2H, $^3J = 6.2$ Hz, CH₂CH₂), 1.91 (s, 6H, N(CH₃)₂), 1.78 (s, 6H, CMe₂Ph), 1.73 (s, 6H, CMe₂Ph), 1.42 (s, 9H, C(CH₃)₃). ¹³C{¹H} NMR (CDCl₃, 100 MHz): δ 156.6, 153.7, 151.5, 142.1, 139.4, 135.2, 132.4, 130.8, 129.7, 127.8, 127.5, 126.8, 126.7, 126.4, 125.7, 125.3, 124.7, 124.6, 122.4 (all Ar-C), 62.3 (CH₃O-Ar), 57.5 (Ar-CH₂-N), 55.9

(N-CH₂-Ar), 53.4 (CH₂CH₂), 50.1 (CH₂CH₂), 45.0 (N(CH₃)₂), 42.4 (CMe₂Ph), 42.0 (CMe₂Ph), 34.9 (C(CH₃)₃), 31.1 (CMe₂Ph), 31.0 (C(CH₃)₃), 29.4 (CMe₂Ph), 21.0 (Ar-CH₃).

2-{N-(3-tert-Butyl-2-methoxy-5-methylbenzyl)-N-[2-(N,N-dimethyl)aminoethyl]aminomethyl]-4,6-dichlorophenol (L⁵H). *N,N*-Dimethylethylenediamine (2.64 g, 30.0 mmol) and a solution of 3-tert-butyl-5-methyl-2-methoxybenzaldehyde (6.18 g, 30.0 mmol) in methanol (20 mL) were heated to reflux for 24 h. After cooling, sodium borohydride (2.28 g, 60.0 mmol) was sequentially added to the above yellow solution at 0 °C to give a viscous oil, to which was added a solution of paraformaldehyde (0.900 g, 30.0 mmol) and 2,4-dichlorophenol (4.89 g, 30.0 mmol) in methanol (20 mL) at 80 °C during 12 h. The mixture was cooled to provide colorless crystals (6.44 g, 45.8%). Anal. Calc. for C₂₄H₃₄Cl₂N₂O₂: C, 63.57; H, 7.56; N, 6.18. Found: C, 63.92; H, 7.98; N, 5.84%. ¹H NMR (CDCl₃, 400 MHz): δ 7.25 (d, 1H, ⁴J = 2.6, ArH), 6.98 (d, 1H, ⁴J = 2.0 Hz, ArH), 6.94 (d, 1H, ⁴J = 2.6 Hz, ArH), 6.92 (d, 1H, ⁴J = 2.0 Hz, ArH), 3.59 (s, 2H, Ar-CH₂-N), 3.58 (s, 5H, CH₃O-Ar and N-CH₂-Ar, overlapped), 2.50 (s, 4H, CH₂CH₂), 2.24 (s, 3H, Ar-CH₃), 2.18 (s, 6H, N(CH₃)₂), 1.35 (s, 9H, C(CH₃)₃). ¹H NMR (C₆D₆, 400 MHz): δ 7.33 (d, 1H, ⁴J = 2.6 Hz, ArH), 7.014 (s, 1H, ArH), 7.011 (s, 1H, ArH), 6.88 (d, 1H, ⁴J = 2.6 Hz, ArH), 3.39 (s, 2H, Ar-CH₂-N), 3.27 (s, 3H, CH₃O-Ar), 3.10 (s, 2H, N-CH₂-Ar), 2.16 (s, 3H, Ar-CH₃), 2.13 (t, 2H, ³J = 6.1 Hz, CH₂CH₂), 1.90 (t, 2H, ³J = 6.1 Hz, CH₂CH₂), 1.82 (s, 6H, N(CH₃)₂), 1.40 (s, 9H, C(CH₃)₃). ¹³C{¹H} NMR (CDCl₃, 100 MHz): δ 156.5, 152.8, 142.3, 132.4, 130.6, 130.0, 128.6, 128.1, 127.1, 126.2, 122.2, 120.0 (all Ar-C), 62.3 (CH₃O-Ar), 55.8 (Ar-CH₂-N), 54.9 (N-CH₂-Ar), 53.0 (CH₂CH₂), 49.4 (CH₂CH₂), 44.7 (N(CH₃)₂), 34.9 (C(CH₃)₃), 31.0 (C(CH₃)₃), 21.0 (Ar-CH₃).

2-{N-(2-Methoxybenzyl)-N-[2-(N,N-dimethyl)aminoethyl]aminomethyl]-4,6-dicumylphenol (L⁶H). The procedure was same as that of L¹H, except that 2, 4-dicumylphenol (9.90 g, 30.0 mmol) were used to afford ligand L⁶H as colorless crystals (5.28 g, 32.0%). Anal. Calc. for C₃₇H₄₆N₂O₂: C, 80.73; H, 8.36; N, 5.09. Found: C, 80.70; H, 8.31; N, 5.01%. ¹H NMR (CDCl₃, 400 MHz): δ 7.29–7.25 (m, 4H, ArH), 7.24–7.20 (m, 6H, ArH), 7.19–7.16 (m, 1H, ArH), 7.15–7.09 (m, 1H, ArH), 6.92 (dd, 1H, ³J = 7.4 Hz, ⁴J = 1.8 Hz, ArH), 6.81–6.78 (m, 2H, ArH), 6.74 (d, 1H, ⁴J = 2.2 Hz, ArH), 3.66 (s, 3H, CH₃O-Ar), 3.62 (s, 2H, Ar-CH₂-N), 3.56 (s, 2H, N-CH₂-Ar), 2.44 (d, 1H, ³J = 7.0 Hz, CH₂CH₂), 2.42 (d, 1H, ³J = 5.5 Hz, CH₂CH₂), 2.19 (d, 1H, ³J = 7.0 Hz, CH₂CH₂), 2.16 (d, 1H, ³J = 5.5 Hz, CH₂CH₂), 2.02 (s, 6H, N(CH₃)₂), 1.69 (s, 6H, CMe₂Ph), 1.67 (s, 6H, CMe₂Ph). ¹³C{¹H} NMR (CDCl₃, 100 MHz): δ 158.1, 153.8, 151.8, 151.6, 139.5, 135.2, 131.7, 128.7, 127.9, 127.6, 126.8, 125.9, 125.8, 125.5, 125.3, 124.6, 122.4, 120.4, 110.3 (all Ar-C), 58.2 (CH₃O-Ar), 56.3 (Ar-CH₂-N), 55.1 (N-CH₂-Ar), 53.1 (CH₂CH₂), 50.5 (CH₂CH₂), 45.5 (N(CH₃)₂), 42.5 (CMe₂Ph), 42.0 (CMe₂Ph), 31.2 (CMe₂Ph), 29.5 (CMe₂Ph).

2-{N-(2-Methoxybenzyl)-N-[2-(N,N-dimethyl)aminoethyl]aminomethyl]-4,6-dichlorophenol (L⁷H). The procedure was same as that of L¹H, except that 2,4-dichlorophenol (4.89 g, 30.0 mmol) were used to afford ligand L⁷H as colorless crystals (3.29 g, 28.6%). Anal. Calc. for C₁₉H₂₄Cl₂N₂O₂: C, 59.53; H, 6.31; N, 7.31. Found: C, 59.30; H, 6.29; N, 7.31%. ¹H NMR (CDCl₃,

400 MHz): δ 7.24 (d, 1H, ⁴J = 2.6 Hz, ArH), 7.23 (td, 1H, ³J = 7.8 Hz, ⁴J = 1.7 Hz, ArH), 7.15 (dd, 1H, ³J = 7.8 Hz, ⁴J = 1.7 Hz, ArH), 6.91 (d, 1H, ⁴J = 2.6 Hz, ArH), 6.88 (td, 1H, ³J = 7.8 Hz, ⁴J = 1.0 Hz, ArH), 6.84 (d, 1H, ³J = 7.8 Hz, ArH), 3.77 (s, 3H, CH₃O-Ar), 3.64 (s, 2H, Ar-CH₂-N), 3.60 (s, 2H, N-CH₂-Ar), 2.57 (d, 1H, ³J = 6.2 Hz, CH₂CH₂), 2.55 (d, 1H, ³J = 6.2 Hz, CH₂CH₂), 2.48 (d, 1H, ³J = 6.2 Hz, CH₂CH₂), 2.46 (d, 1H, ³J = 6.2 Hz, CH₂CH₂), 2.13 (s, 6H, N(CH₃)₂). ¹³C{¹H} NMR (CDCl₃, 100 MHz): δ 158.0, 152.8, 131.5, 128.9, 128.4, 127.7, 126.0, 125.1, 122.4, 121.6, 120.1, 110.3 (all Ar-C), 55.9 (CH₃O-Ar), 55.6 (Ar-CH₂-N), 55.0 (N-CH₂-Ar), 52.9 (CH₂CH₂), 49.7 (CH₂CH₂), 44.9 (N(CH₃)₂).

6-tert-Butyl-2-{N-(2-(N,N-dimethylamino)-5-methylbenzyl)-N-[2-(N,N-dimethyl)aminoethyl]aminomethyl]-4-methylphenol (L⁸H). *N,N*-Dimethylethylenediamine (2.64 g, 30.0 mmol) and a solution of 2-(N,N-dimethylamino)-5-methylbenzaldehyde (4.89 g, 30.0 mmol) in methanol (20 mL) were heated to reflux for 24 h. After cooling, sodium borohydride (2.28 g, 60.0 mmol) was sequentially added to the above yellow solution at 0 °C to give a viscous oil, to which was added a solution of paraformaldehyde (0.900 g, 30.0 mmol) and 2-tert-butyl-4-methylphenol (4.92 g, 30.0 mmol) in methanol (20 mL) at 80 °C during 12 h. The mixture was cooled to provide ligand L⁸H as white solids (3.74 g, 30.4%). Anal. Calc. for C₂₆H₄₁N₃O: C, 75.87; H, 10.04; N, 10.21. Found: C, 75.86; H, 9.96; N, 10.11. ¹H NMR (CDCl₃, 400 MHz): δ 7.21 (s, 1H, ArH), 6.994 (s, 1H, ArH), 6.991 (s, 1H, ArH), 6.98 (d, 1H, ⁴J = 1.8 Hz, ArH), 6.71 (d, 1H, ⁴J = 1.8 Hz, ArH), 3.72 (s, 2H, Ar-CH₂-N), 3.66 (s, 2H, N-CH₂-Ar), 2.61 (s, 6H, (CH₃)₂N-Ar), 2.55–2.52 (m, 2H, CH₂CH₂), 2.46–2.42 (m, 2H, CH₂CH₂), 2.26 (s, 3H, Ar-CH₃), 2.24 (s, 3H, Ar-CH₃), 2.13 (s, 6H, N(CH₃)₂), 1.45 (s, 9H, C(CH₃)₃). ¹H NMR (C₆D₆, 400 MHz): δ 10.89 (s, 1H, OH), 7.47 (s, 1H, ArH), 7.22 (s, 1H, ArH), 6.92 (d, 1H, ³J = 8.1 Hz, ArH), 6.86 (d, 1H, ³J = 8.1 Hz, ArH), 6.76 (s, 1H, ArH), 3.71 (s, 2H, Ar-CH₂-N), 3.59 (s, 2H, N-CH₂-Ar), 2.43 (t, 2H, ³J = 6.4 Hz, CH₂CH₂), 2.38 (s, 6H, (CH₃)₂N-Ar), 2.27 (s, 3H, Ar-CH₃), 2.25 (s, 3H, Ar-CH₃), 2.19 (t, 2H, ³J = 6.4 Hz, CH₂CH₂), 1.94 (s, 6H, N(CH₃)₂), 1.72 (s, 9H, C(CH₃)₃). ¹³C{¹H} NMR (CDCl₃, 100 MHz): δ 154.2, 151.0, 136.3, 132.8, 132.5, 131.6, 128.3, 127.8, 126.5, 126.4, 123.1, 119.0 (all Ar-C), 57.8 (Ar-CH₂-N), 56.4 (N-CH₂-Ar), 52.8 (CH₂CH₂), 50.6 (CH₂CH₂), 45.5 ((CH₃)₂N-Ar), 45.3 (R-N(CH₃)₂), 34.6 (C(CH₃)₃), 29.6 (C(CH₃)₃), 20.8 (Ar-CH₃), 20.7 (Ar-CH₃).

2-{N-(2-(N,N-Dimethylamino)-5-methylbenzyl)-N-[2-(N,N-dimethyl)aminoethyl]aminomethyl]-4,6-dicumylphenol (L⁹H). The procedure was same as that of L⁸H, except that 2,4-dicumylphenol (9.90 g, 30.0 mmol) were used to provide ligand L⁹H as viscous oil (4.05 g, 23.4%). Anal. Calc. for C₃₉H₅₁N₃O: C, 81.06; H, 8.90; N, 7.27. Found: C, 81.14; H, 8.95; N, 7.11%. ¹H NMR (CDCl₃, 400 MHz): δ 7.27–7.06 (m, 10H, ArH), 7.09 (tt, 1H, ³J = 6.7 Hz, ⁴J = 1.7 Hz, ArH), 6.98 (s, 2H, ArH), 6.94 (s, 1H, ArH), 6.76 (d, 1H, ⁴J = 2.2 Hz, ArH), 3.60 (s, 2H, Ar-CH₂-N), 3.58 (s, 2H, N-CH₂-Ar), 2.53 (s, 6H, (CH₃)₂N-Ar), 2.41 (d, 1H, ³J = 6.6, CH₂CH₂), 2.39 (d, 1H, ³J = 5.5, CH₂CH₂), 2.24 (d, 1H, ³J = 5.5, CH₂CH₂), 2.22 (d, 1H, ³J = 6.6, CH₂CH₂), 2.21 (s, 3H, Ar-CH₃), 2.03 (s, 6H, N(CH₃)₂), 1.70 (s, 6H, CMe₂Ph), 1.69 (s, 6H, CMe₂Ph). ¹³C{¹H} NMR (CDCl₃, 100 MHz): δ 153.7, 151.6, 151.5, 150.9, 139.3, 135.1, 132.7, 132.1, 131.4, 128.4, 127.8, 127.4, 126.7, 126.1, 125.7, 125.3, 124.6, 124.5, 122.5, 119.1 (all

Ar-C), 58.0 (Ar-CH₂-N), 56.1 (N-CH₂-Ar), 53.3 (CH₂CH₂), 50.3 (CH₂CH₂), 45.3 ((CH₃)₂N-Ar), 45.2 (R-N(CH₃)₂), 42.4 (CMe₂Ph), 42.0 (CMe₂Ph), 31.1 (CMe₂Ph), 29.4 (CMe₂Ph), 20.7 (Ar-CH₃).

2-{N-(2-(N,N-Dimethylamino)-5-methylbenzyl)-N-[2-(N,N-dimethylaminoethyl)aminomethyl]-4,6-dichlorophenol (L¹⁰H).

The procedure was same as that of L⁸H, except that 2,4-dichlorophenol (4.89 g, 30.0 mmol) were used to afford ligand L¹⁰H as colorless crystals (3.80 g, 30.9%). Anal. Calc. for C₂₁H₂₉Cl₂N₃O: C, 61.46; H, 7.07; N, 10.24. Found: C, 61.37; H, 7.01; N, 10.18%. ¹H NMR (CDCl₃, 400 MHz): δ 7.24 (d, 1H, ⁴J = 2.6 Hz, ArH), 7.07 (s, 1H, ArH), 6.98 (s, 2H, ArH), 6.93 (d, 1H, ⁴J = 2.6 Hz, ArH), 3.63 (s, 2H, Ar-CH₂-N), 3.62 (s, 2H, N-CH₂-Ar), 2.56 (s, 6H, (CH₃)₂N-Ar), 2.54–2.47 (m, 4H, CH₂CH₂), 2.17 (s, 6H, R-N(CH₃)₂). ¹H NMR (C₆D₆, 400 MHz): δ 7.30 (d, 1H, ⁴J = 2.6 Hz, ArH), 7.15 (s, 1H, ArH, overlapped with C₆D₆ signal), 6.7 (dd, 1H, ³J = 8.1 Hz, ⁴J = 1.8 Hz, ArH), 6.84 (s, 1H, ArH), 6.82 (d, 1H, ³J = 8.1 Hz, ArH overlapped), 3.50 (s, 2H, Ar-CH₂-N), 3.17 (s, 2H, N-CH₂-Ar), 2.38 (s, 6H, (CH₃)₂N-Ar), 2.21 (t, 2H, ³J = 6.1 Hz, CH₂CH₂), 2.16 (s, 3H, ArCH₃), 1.97 (t, 2H, ³J = 6.1 Hz, CH₂CH₂), 1.83 (s, 6H, R-N(CH₃)₂). ¹³C{¹H} NMR (CDCl₃, 100 MHz): δ 152.8, 151.0, 132.6, 131.8, 131.5, 128.6, 128.5, 127.9, 126.3, 122.3, 121.8, 119.1 (all Ar-C), 55.9 (Ar-CH₂-N), 55.4 (N-CH₂-Ar), 53.2 (CH₂CH₂), 49.6 (CH₂CH₂), 45.4 ((CH₃)₂N-Ar), 44.8 (R-N(CH₃)₂), 20.7 (Ar-CH₃).

[(L¹)ZnN(SiMe₃)₂] (1). The ligand L¹H (0.384 g, 1.00 mmol) was added slowly to a solution of Zn[N(SiMe₃)₂]₂ (0.385 g, 1.00 mmol) in light petroleum (20 mL). The solution was stirred for 24 h at r.t. and white solids precipitated. The mixture was filtered and the solids were dried under vacuum for several hours. The white powder obtained was then dissolved with 10 mL of toluene and filtered. The clear filtrate was concentrated and kept at -40 °C to give colorless crystals (465 mg, 75%, two crops). Anal. Calc. for C₃₀H₅₃N₃O₂Si₂Zn: C, 59.21; H, 8.72; N, 6.91. Found: C, 59.43; H, 8.86; N, 6.95%. ¹H NMR (C₆D₆, 400 MHz): δ 7.31 (d, 1H, ⁴J = 2.0 Hz, ArH), 7.10 (td, 1H, ³J = 8.0 Hz, ⁴J = 1.6 Hz, ArH), 6.97 (dd, 1H, ³J = 7.6 Hz, ⁴J = 1.6 Hz, ArH), 6.80 (td, 1H, ³J = 7.6 Hz, ⁴J = 0.8 Hz, ArH), 6.48 (d, 1H, ³J = 8.0 Hz, ArH), 6.41 (d, 1H, ⁴J = 2.0 Hz, ArH), 4.40 (d, 1H, ²J = 14.0 Hz, Ar-CH₂-N), 4.24 (d, 1H, ²J = 12.0 Hz, N-CH₂-Ar), 4.13 (d, 1H, ²J = 14.0 Hz, Ar-CH₂-N), 3.31 (d, 1H, ²J = 12.0 Hz, N-CH₂-Ar), 3.11 (s, 3H, CH₃O-Ar), 2.45 (m, 2H, CH₂CH₂), 2.23 (s, 3H, Ar-CH₃), 2.21 (m, 1H, CH₂CH₂), 1.93 (br s, 6H, N(CH₃)₂), 1.77 (s, 9H, C(CH₃)₃), 1.60–1.57 (m, 1H, CH₂CH₂), 0.56 (s, 18H, N(Si(CH₃)₃)₂). ¹³C{¹H} NMR (C₆D₆, 100 MHz): δ 164.9, 159.0, 138.6, 134.5, 130.6, 130.4, 128.9, 120.9, 120.8, 120.4, 111.2 (all Ar-C), 59.6 (CH₃O-Ar), 58.0 (Ar-CH₂-N), 54.9 (N-CH₂-Ar), 52.8 (CH₂CH₂), 47.6 (N(CH₃)₂), 45.6 (CH₂CH₂), 35.5 (C(CH₃)₃), 30.5 (C(CH₃)₃), 20.9 (Ar-CH₃), 7.4 (Si(CH₃)₃).

[(L²)ZnN(SiMe₃)₂] (2). Following a procedure similar to that described for 1, L²H (0.426 g, 1.00 mmol) was treated with Zn[N(SiMe₃)₂]₂ (0.385 g, 1.00 mmol) in light petroleum (20 mL) at r.t. to obtain white solids. Recrystallization with toluene afforded colorless crystals (403 mg, 62%, two crops). Anal. Calc. for C₃₃H₅₉N₃O₂Si₂Zn: C, 60.92; H, 9.07; N, 6.46. Found: C, 60.71; H, 9.28; N, 6.42%. ¹H NMR (C₆D₆, 400 MHz): δ 7.60 (d, 1H, ⁴J

= 2.5 Hz, ArH), 7.08–7.02 (m, 2H, ArH), 6.78 (d, 1H, ⁴J = 2.5 Hz, ArH), 6.77 (t, 1H, ³J = 7.4 Hz, ArH), 6.43 (d, 1H, ³J = 8.2 Hz, ArH), 4.43 (d, 1H, ²J = 14.0 Hz, Ar-CH₂-N), 4.27 (d, 1H, ²J = 12.4 Hz, N-CH₂-Ar), 4.15 (d, 1H, ²J = 14.0 Hz, Ar-CH₂-N), 3.44 (d, 1H, ²J = 12.4 Hz, N-CH₂-Ar), 3.10 (s, 3H, CH₃O-Ar), 2.56–2.43 (m, 2H, CH₂CH₂), 2.35–2.31 (m, 1H, CH₂CH₂), 1.92 (br s, 6H, N(CH₃)₂), 1.81 (s, 9H, C(CH₃)₃), 1.62–1.58 (m, 1H, CH₂CH₂), 1.32 (s, 9H, C(CH₃)₃), 0.56 (s, 18H, N(Si(CH₃)₃)₂). ¹³C{¹H} NMR (C₆D₆, 100 MHz): δ 164.8, 158.9, 138.2, 134.8, 134.5, 130.3, 126.5, 124.9, 120.9, 120.4, 111.3 (all Ar-C), 60.2 (CH₃O-Ar), 57.9 (Ar-CH₂-N), 54.8 (N-CH₂-Ar), 52.8 (CH₂CH₂), 46.0 (CH₂CH₂), 35.9 (C(CH₃)₃), 34.0 (C(CH₃)₃), 32.2 (C(CH₃)₃), 30.5 (C(CH₃)₃), 7.4 (Si(CH₃)₃).

[(L³)ZnN(SiMe₃)₂] (3). Following a procedure similar to that described for 1, L³H (0.454 g, 1.00 mmol) was treated with Zn[N(SiMe₃)₂]₂ (0.385 g, 1.00 mmol) in light petroleum (20 mL) at r.t. to obtain white solids. Recrystallization with toluene afforded colorless crystals (468 mg, 69%, two crops). Anal. Calc. for C₃₅H₆₃N₃O₂Si₂Zn: C, 61.95; H, 9.29; N, 6.19. Found: C, 61.49; H, 9.46; N, 5.77%. ¹H NMR (C₆D₆, 400 MHz): δ 7.29 (d, 1H, ⁴J = 2.0 Hz, ArH), 7.15 (br s, 1H, ArH, overlapped with C₆D₆ signal), 6.82 (d, 1H, ⁴J = 1.6 Hz, ArH), 6.36 (d, 1H, ⁴J = 1.6 Hz, ArH), 4.28 (d, 1H, ²J = 14.0 Hz, Ar-CH₂-N), 4.20 (d, 1H, ²J = 12.4 Hz, N-CH₂-Ar), 4.11 (d, 1H, ²J = 14.0 Hz, Ar-CH₂-N), 3.33 (s, 3H, CH₃O-Ar), 3.23 (d, 1H, ²J = 12.4 Hz, N-CH₂-Ar), 2.49–2.30 (m, 3H, CH₂CH₂), 2.16 (s, 3H, Ar-CH₃), 2.15 (s, 3H, Ar-CH₃), 2.04 (br s, 3H, NCH₃), 1.77 (s, 9H, C(CH₃)₃), 1.74 (br s, 3H, NCH₃), 1.61–1.55 (m, 1H, CH₂CH₂), 1.36 (s, 9H, C(CH₃)₃), 0.59 (s, 18H, N(Si(CH₃)₃)₂). ¹³C{¹H} NMR (C₆D₆, 100 MHz): δ 164.8, 158.0, 143.4, 138.5, 133.3, 132.9, 130.7, 129.6, 128.9, 125.0, 121.1, 120.9 (all Ar-C), 63.3 (CH₃O-Ar), 59.6 (Ar-CH₂-N), 58.2 (N-CH₂-Ar), 53.9 (CH₂CH₂), 45.6 (CH₂CH₂), 35.5 (C(CH₃)₃), 35.1 (C(CH₃)₃), 31.3 (C(CH₃)₃), 30.5 (C(CH₃)₃), 21.1 (Ar-CH₃), 20.8 (Ar-CH₃), 7.6 (Si(CH₃)₃).

[(L⁴)ZnN(SiMe₃)₂] (4). An analogous method to that of 1 was utilized, except that L⁴H (0.636 g, 1.00 mmol) and Zn[N(SiMe₃)₂]₂ (0.385 g, 1.00 mmol) were used to give colorless crystals (559 mg, 65%, two crops). Anal. Calc. for C₄₈H₇₃N₃O₂Si₂Zn: C, 68.17; H, 8.70; N, 4.97. Found: C, 67.76; H, 8.75; N, 4.47%. ¹H NMR (C₆D₆, 400 MHz): δ 7.55 (d, 2H, ³J = 7.6 Hz, CMe₂Ph), 7.52 (d, 1H, ⁴J = 2.0 Hz, ArH), 7.29 (d, 2H, ³J = 8.0 Hz, CMe₂Ph), 7.17 (t, 2H, ³J = 7.6 Hz, CMe₂Ph), 7.12 (t, 2H, ³J = 7.6 Hz, CMe₂Ph), 7.07 (s, 1H, ArH), 7.01 (m, 2H, CMe₂Ph), 6.80 (s, 1H, ArH), 6.68 (d, 1H, ⁴J = 2.0 Hz, ArH), 4.33 (d, 1H, ²J = 12.8 Hz, Ar-CH₂-N), 4.11 (s, 2H, N-CH₂-Ar), 3.31 (s, 3H, CH₃O-Ar), 3.28 (d, 1H, Ar-CH₂-N, partially overlapped with CH₃O-Ar signal), 2.38 (m, 2H, CH₂CH₂), 2.18 (s, 3H, Ar-CH₃), 2.09 (s, 3H, CMe₂Ph), 2.07 (m, 1H, CH₂CH₂), 1.91 (br s, 3H, N(CH₃)₂), 1.73 (s, 3H, CMe₂Ph), 1.64 (br s, 1H, CH₂CH₂), 1.61 (s, 3H, CMe₂Ph), 1.59 (s, 3H, CMe₂Ph), 1.33 (s, 9H, C(CH₃)₃), 1.14 (br s, 3H, N(CH₃)₂), 0.48 (s, 18H, N(Si(CH₃)₃)₂). ¹³C{¹H} NMR (C₆D₆, 100 MHz): δ 164.3, 157.9, 152.4, 143.4, 137.6, 133.9, 132.9, 132.8, 129.6, 127.3, 127.1, 125.4, 125.1, 124.6, 120.4, 100.2 (all Ar-C), 63.2 (CH₃O-Ar), 60.6 (Ar-CH₂-N), 58.3 (N-CH₂-Ar), 54.6 (CH₂CH₂), 46.2 (CH₂CH₂), 42.8 (CMe₂Ph), 42.4 (CMe₂Ph), 35.0 (C(CH₃)₃), 33.5, (CMe₂Ph), 31.42 (CMe₂Ph), 31.37 (CMe₂Ph), 31.3 (C(CH₃)₃), 27.0 (CMe₂Ph), 21.1 (Ar-CH₃), 7.5 (Si(CH₃)₃).

[(L⁵)ZnN(SiMe₃)₂] (5). An analogous method to that of **1** was utilized, except that L⁵H (0.469 g, 1.00 mmol) and Zn[N(SiMe₃)₂]₂ (0.385 g, 1.00 mmol) were used to give colorless crystals (413 mg, 61%). Anal. Calc. for C₃₀H₅₁Cl₂N₃O₂Si₂Zn·1/4(C₇H₈): C, 54.43; H, 7.57; N, 6.00. Found: C, 54.22; H, 7.74; N, 5.88%. ¹H NMR (C₆D₆, 400 MHz): δ 7.43 (d, 1H, ⁴J = 2.4 Hz, ArH), 7.15 (br s, 1H, ArH, overlapped with C₆D₆ signal), 6.83 (s, 1H, ArH), 6.37 (d, 1H, ⁴J = 2.4 Hz, ArH), 4.13 (d, 1H, ²J = 14.0 Hz, N-CH₂-Ar), 3.96 (d, 1H, ²J = 14.0 Hz, N-CH₂-Ar), 3.92 (d, 1H, ²J = 12.8 Hz, Ar-CH₂-N), 3.29 (s, 3H, CH₃O-Ar), 2.88 (d, 1H, ²J = 12.8 Hz, Ar-CH₂-N), 2.19 (s, 3H, Ar-CH₃), 2.16–2.11 (m, 2H, CH₂CH₂), 2.10 (s, 0.72 H, CH₃-C₆H₅), 2.01 (br s, 3H, NCH₃), 1.96–1.93 (m, 1H, CH₂CH₂), 1.71 (br s, 3H, NCH₃), 1.53–1.50 (m, 1H, CH₂CH₂), 1.36 (s, 9H, C(CH₃)₃), 0.54 (s, 18H, N(Si(CH₃)₃)₂). ¹³C{¹H} NMR (C₆D₆, 100 MHz): δ 161.8, 157.7, 143.5, 133.3, 132.4, 130.3, 129.8, 129.4, 125.7, 124.8, 123.7, 116.9, (all Ar-C), 63.1 (CH₃O-Ar), 58.7 (Ar-CH₂-N), 57.4 (N-CH₂-Ar), 55.0 (CH₂CH₂), 48.2 (N(CH₃)₂), 47.2 (CH₂CH₂), 45.1 (N(CH₃)₂), 35.1 (C(CH₃)₃), 31.4 (C(CH₃)₃), 21.2 (Ar-CH₃), 20.8 (Ar-CH₃), 7.10 (Si(CH₃)₃).

[(L⁶)ZnEt] (6). L⁶H (0.643 g, 1.00 mmol) was dissolved in toluene (10 mL) and cooled to -40 °C. Diethyl zinc (1.00 mL, 1.00 mmol, 1 M in hexane) was added to this solution and the colorless mixture was stirred for 12 h at room temperature. White solids were afforded by solvent evaporation under vacuum, which were further dried under high vacuum for several hours. The solids were then recrystallized with toluene and kept at -40 °C to give colorless crystals (508 mg, 79%). Anal. Calc. for C₃₉H₅₀N₂O₂Zn·1/2(C₇H₈): C, 74.02; H, 7.84; N, 4.06. Found: C, 73.64; H, 8.08; N, 3.79%. ¹H NMR (CDCl₃, 400 MHz): δ 7.47 (dd, 2H, ³J = 8.4 Hz, ⁴J = 1.2 Hz, CMe₂Ph), 7.35 (td, 1H, ³J = 7.8 Hz, ⁴J = 2.0 Hz, ArH), 7.26 (d, 1H, ³J = 7.2 Hz, ArH, overlapped with CDCl₃ signal), 7.23–7.15 (m, 8H, CMe₂Ph), 7.06 (t, 1H, ³J = 7.3 Hz, CMe₂Ph), 6.97 (td, 1H, ³J = 7.4 Hz, ⁴J = 0.8 Hz, ArH), 6.92 (d, 1H, ³J = 8.4 Hz, ArH), 6.51 (d, 1H, ⁴J = 2.8 Hz, ArH), 4.14 (d, 1H, ²J = 14.0 Hz, Ar-CH₂-N), 4.07 (d, 1H, ²J = 11.6 Hz, N-CH₂-Ar), 3.92, (d, 1H, ²J = 14.0 Hz, Ar-CH₂-N), 3.78 (s, 3H, CH₃O-Ar), 3.12 (d, 1H, ²J = 11.6 Hz, N-CH₂-Ar), 2.57–2.46 (m, 2H, CH₂CH₂), 2.37 (s, 1.5 H, CH₃-C₆H₅), 2.36–2.31 (m, 1H, CH₂CH₂), 2.02 (very br, 3H, NCH₃), 1.95 (s, 3H, CMe₂Ph), 1.93–1.88 (m, 1H, CH₂CH₂), 1.65 (s, 3H, CMe₂Ph), 1.63 (s, 3H, CMe₂Ph), 1.62 (s, 3H, CMe₂Ph), 1.32 (t, 3H, ³J = 8.1 Hz, CH₂CH₃), 1.02 (very br, 3H, NCH₃), 0.14 (dq, 1H, ²J = 12.9 Hz, ³J = 8.1 Hz, CH₂CH₃), 0.05 (dq, 1H, ²J = 12.9 Hz, ³J = 8.1 Hz, CH₂CH₃). ¹³C{¹H} NMR (CDCl₃, 100 MHz): δ 165.1, 158.5, 152.7, 150.8, 136.4, 133.9, 133.4, 129.9, 128.2, 127.5, 126.9, 126.7, 125.7, 124.9, 124.2, 122.0, 120.9, 120.3, 110.8 (all Ar-C), 59.0 (CH₃O-Ar), 57.4 (Ar-CH₂-N), 55.2 (N-CH₂-Ar), 52.5 (CH₂CH₂), 45.4 (CH₂CH₂), 42.1 (CMe₂Ph), 41.9 (CMe₂Ph), 31.2, (CMe₂Ph), 31.11 (CMe₂Ph), 31.06 (CMe₂Ph), 26.5 (CMe₂Ph), 13.2 (CH₂CH₃), 3.60 (CH₂CH₃).

[(L⁷)ZnEt] (7). An analogous method to that of **6** was utilized, except that L⁷H (0.383 g, 1.00 mmol) and diethyl zinc (1.00 mL, 1.00 mmol, 1 M in hexane) were used to give colorless crystals (362 mg, 76%). Anal. Calc. for C₂₁H₂₈Cl₂N₂O₂Zn: C, 52.91; H, 6.08; N, 5.88. Found: C, 52.97; H, 6.03; N, 5.71%. ¹H NMR (CDCl₃, 400 MHz): δ 7.39 (td, 1H, ³J = 8.2 Hz, ⁴J = 1.7 Hz, ArH), 7.27 (dd, 1H, ³J = 7.4 Hz, ⁴J = 1.7 Hz, ArH), 7.24 (d, 1H, ⁴J = 2.7 Hz, ArH), 7.02 (td, 1H, ³J = 7.4 Hz, ⁴J = 1.0 Hz, ArH),

6.97 (d, 1H, ³J = 8.2 Hz, ArH), 6.67 (d, 1H, ⁴J = 2.7 Hz, ArH), 4.30 (d, 1H, ²J = 14.0 Hz, Ar-CH₂-N), 4.16 (d, 1H, ²J = 12.0 Hz, N-CH₂-Ar), 3.98 (d, 1H, ²J = 14.0 Hz, Ar-CH₂-N), 3.83 (s, 3H, CH₃O-Ar), 3.32 (d, 1H, ²J = 12.0 Hz, N-CH₂-Ar), 2.74–2.63 (m, 2H, CH₂CH₂), 2.42–2.35 (m, 1H, CH₂CH₂), 2.39 (br, 3H, NCH₃), 2.18–2.12 (m, 1H, CH₂CH₂), 2.15 (br, 3H, NCH₃), 1.33 (t, 3H, ³J = 8.0 Hz, CH₂CH₃), 0.29 (qd, 2H, ³J = 8.0 Hz, ²J = 1.3 Hz, CH₂CH₃). ¹³C{¹H} NMR (CDCl₃, 100 MHz): δ 161.4, 158.4, 133.7, 130.4, 129.5, 129.3, 134.9, 124.8, 120.5, 120.0, 116.7, 111.1 (all Ar-C), 57.9 (CH₃O-Ar), 57.6 (Ar-CH₂-N), 55.3 (N-CH₂-Ar), 53.2 (CH₂CH₂), 46.2 (CH₂CH₂), 13.3 (CH₂CH₃), 3.60 (CH₂CH₃).

[(L⁸)ZnN(SiMe₃)₂] (8). An analogous method to that of **1** was utilized, except that L⁸H (0.411 g, 1.00 mmol) and Zn[N(SiMe₃)₂]₂ (0.385 g, 1.00 mmol) were used to give colorless crystals (426 mg, 67%, two crops from hexane). Anal. Calc. for C₃₂H₅₈N₄O₂Si₂Zn·1/4(C₆H₁₄): C, 61.10; H, 9.35; N, 8.51. Found: C, 60.93; H, 9.35; N, 8.71. ¹H NMR (CDCl₃, 400 MHz): δ 7.30 (d, 1H, ArH), 6.97 (d, 1H, ³J = 8.0 Hz, ArH), 6.94 (s, 1H, ArH), 6.93 (d, 1H, ³J = 8.0 Hz, ArH), 6.40 (s, 1H, ArH), 4.52 (d, 1H, ²J = 13.6 Hz, Ar-CH₂-N), 4.28 (br d, 1H, ²J = 11.3 Hz, N-CH₂-Ar), 4.06 (br d, 1H, ²J = 13.6 Hz, Ar-CH₂-N), 3.34 (br d, 1H, ²J = 11.3 Hz, N-CH₂-Ar), 2.54 (t, 1H, ²J = 12.8 Hz, CH₂CH₂), 2.44 (t, 1H, ²J = 12.8 Hz, CH₂CH₂), 2.37–2.32 (m, 1H, CH₂CH₂), 2.27 (s, 6H, Ar-N(CH₃)₂), 2.22 (s, 3H, Ar-CH₃), 2.12 (s, 3H, Ar-CH₃), 2.06 (br s, 3H, N(CH₃)₂), 1.81 (br s, 3H, N(CH₃)₂), 1.77 (s, 9H, C(CH₃)₃), 1.63 (d, 1H, ²J = 10.3 Hz, CH₂CH₂), 1.22–1.28 [m, 2 H, CH₃(CH₂)₄CH₃] 0.88 [t, 1.5H, ³J = 6.8, CH₃(CH₂)₄CH₃], 0.57 (s, 18H, N(Si(CH₃)₃)₂). ¹³C{¹H} NMR (C₆D₆, 100 MHz): δ 164.8, 159.0, 138.3, 134.6, 133.9, 130.6, 130.5, 128.6, 121.2, 120.8, 120.6 (all Ar-C), 59.6 (Ar-CH₂-N), 58.0 (N-CH₂-Ar), 53.4 (CH₂CH₂), 45.7 (CH₂CH₂), 35.3 (N(CH₃)₂), 31.7 (C(CH₃)₃), 30.3 (C(CH₃)₃), 20.7 (Ar-CH₃), 7.3 (Si(CH₃)₃).

[(L⁹)ZnEt] (9). An analogous method to that of **6** was utilized, except that L⁹H (0.577 g, 1.00 mmol) and diethyl zinc (1.00 mL, 1.00 mmol, 1 M in hexane) were used to give colorless crystals (542 mg, 80%). Anal. Calc. for C₄₁H₅₅N₃OZn: C, 73.43; H, 8.21; N, 6.27. Found: C, 73.22; H, 8.21; N, 6.07%. ¹H NMR (CDCl₃, 400 MHz): δ 7.45 (d, 2H, ³J = 7.3 Hz, CMe₂Ph), 7.21–7.07 (m, 11H, ArH), 7.05 (t, 1H, ³J = 7.3 Hz, CMe₂Ph), 6.52 (d, 1H, ⁴J = 2.5 Hz, ArH), 4.27 (d, 1H, ²J = 13.6 Hz, Ar-CH₂-N), 4.06 (d, 1H, ²J = 11.9 Hz, N-CH₂-Ar), 3.80 (d, 1H, ²J = 13.6 Hz, Ar-CH₂-N), 3.12 (d, 1H, ²J = 11.9 Hz, N-CH₂-Ar), 2.54 (s, 6H, Ar-N(CH₃)₂), 2.54–2.43 (m, 2H, CH₂CH₂ overlapped with Ar-CH₃), 2.32 (s, 3H, Ar-CH₃), 2.29–2.23 (m, 1H, CH₂CH₂), 1.94 (s, 3H, CMe₂Ph), 1.84–1.80 (m, 1H, CH₂CH₂), 1.63 (s, 3H, CMe₂Ph), 1.62 (s, 3H, CMe₂Ph), 1.61 (s, 3H, CMe₂Ph), 1.49 (br s, 6H, N(CH₃)₂), 1.32 (t, 3H, ³J = 8.1 Hz, CH₂CH₃), 0.15 (dq, 1H, ²J = 12.9 Hz, ³J = 8.1 Hz, CH₂CH₃), 0.06 (dq, 1H, ²J = 12.9 Hz, ³J = 8.1 Hz, CH₂CH₃). ¹³C{¹H} NMR (CDCl₃, 100 MHz): δ 165.2, 152.7, 152.3, 150.8, 136.4, 134.0, 133.6, 133.3, 130.2, 128.1, 128.0, 127.5, 127.4, 126.9, 126.7, 125.9, 124.9, 124.1, 122.2, 120.7 (all Ar-C), 59.4 (Ar-CH₂-N), 57.7 (N-CH₂-Ar), 53.3 (CH₂CH₂), 45.7 (Ar-N(CH₃)₂), 45.3 (R-N(CH₃)₂), 45.1 (CH₂CH₂), 42.1 (CMe₂Ph), 41.9 (CMe₂Ph), 31.2, (CMe₂Ph), 31.1 (CMe₂Ph), 31.07 (CMe₂Ph), 26.6 (CMe₂Ph), 20.9 (Ar-CH₃), 13.3 (CH₂CH₃), 3.28 (CH₂CH₃).

[(L¹⁰)ZnEt] (**10**). An analogous method to that of **6** was utilized, except that L¹⁰H (0.410 g, 1.00 mmol) and diethyl zinc (1.00 mL, 1.00 mmol, 1 M in hexane) were used to give colorless crystals (458 mg, 91%, two crops). Anal. Calc. for C₂₃H₃₃Cl₂N₃OZn: C, 54.87; H, 6.56; N, 8.35. Found: C, 55.10; H, 6.58; N, 8.31%. ¹H NMR (CDCl₃, 400 MHz): δ 7.23 (d, 1H, ⁴J = 2.7 Hz, ArH), 7.18 (s, 2H, ArH), 7.10 (s, 1H, ArH), 6.67 (d, 1H, ⁴J = 2.7 Hz, ArH), 4.42 (d, 1H, ²J = 13.6 Hz, Ar-CH₂-N), 3.91 (d, 1H, ²J = 12.4 Hz, N-CH₂-Ar), 3.98 (d, 1H, ²J = 13.6 Hz, Ar-CH₂-N), 3.34 (d, 1H, ²J = 12.4 Hz, N-CH₂-Ar), 2.77 (ddd, 1H, ²J = 12.6 Hz, ³J = 5.6 Hz, ³J = 4.0 Hz, CH₂CH₂), 2.69–2.62 (m, 1H, CH₂CH₂), 2.60 (s, 6H, Ar-N(CH₃)₂), 2.36 (s, 3H, Ar-CH₃), 2.34–2.28 (m, 1H, CH₂CH₂), 2.26 (s, 6H, R-N(CH₃)₂), 2.12 (ddd, 1H, ²J = 12.6 Hz, ³J = 5.6 Hz, ³J = 4.0 Hz, CH₂CH₂), 1.34 (t, 3H, ³J = 8.0 Hz, CH₂CH₃), 0.314 (qd, 2H, ³J = 8.0 Hz, ²J = 2.2 Hz, CH₂CH₃). ¹³C{¹H} NMR (CDCl₃, 100 MHz): δ 161.5, 152.3, 133.8, 130.6, 129.5, 129.5, 129.3, 127.0, 125.1, 124.8, 121.0, 116.6 (all Ar-C), 58.1 (Ar-CH₂-N), 57.9 (N-CH₂-Ar), 54.0 (CH₂CH₂), 46.1 (Ar-N(CH₃)₂), 45.9 (CH₂CH₂), 45.7 (R-N(CH₃)₂), 20.9 (Ar-CH₃), 13.4 (CH₂CH₃), 3.49 (CH₂CH₃).

Typical polymerization experiments

In a Braun Labstar glove-box, an initiator solution from a stock solution in THF or toluene was injected sequentially to a series of 10 mL vials loaded with *rac*-lactide and suitable amounts of dry solvent. After specified time intervals, each vial was taken out of the glove-box; an aliquot was withdrawn and quenched quickly with light petroleum, the reaction mixture was quenched at the same time by adding an excess amount of light petroleum and one drop of water. All the volatiles in the aliquots were removed and the residue was subjected to monomer conversion determination which was monitored by integration of monomer vs. polymer methine or methyl resonances in ¹H NMR (CDCl₃, 400 MHz). The precipitates collected from the bulk mixture were dried in air, dissolved with dichloromethane and sequentially precipitated into light petroleum ether. The obtained polymer was further dried in a vacuum oven at 50 °C for 16 h. Each reaction was used as one data point. In the cases where 2-propanol was used, the solution of initiator was injected to the solution of *rac*-lactides in toluene or THF to which 2-propanol was added. Otherwise the procedures were the same.

X-Ray crystallography

Suitable crystals of complexes **1**, **3**, **7**, **9** and **10** for X-ray analysis were obtained from the saturated toluene, n-hexane solution or toluene–pentane mixture, respectively, at –40 °C or room temperature. Diffraction data were collected on a Bruker AXSD 8 diffractometer for complexes **1**, **7** and **10** and Bruker SMART APEX II diffractometer for complexes **3** and **9** with graphite-monochromated Mo-Kα (λ = 0.71073 Å) radiation. All data were collected at 20 °C using the ω-scan techniques. All structures were solved by direct methods and refined using Fourier techniques. An absorption correction based on SADABS was applied.⁵⁹ All non-hydrogen atoms were refined by full-matrix least-squares on F² using the SHELXTL program package.⁶⁰ Hydrogen atoms were located and refined by the geometry method. The cell refinement, data collection, and reduction

were done by Bruker SAINT.⁶¹ The structure solution and refinement were performed by SHELXS-97⁶² and SHELXL-97⁶³ respectively. For further crystal data and details of measurements see Tables 2–4. Molecular structures were generated using ORTEP program.⁶⁴

Acknowledgements

This work is subsidized by the National Basic Research Program of China (2005CB623801), National Natural Science Foundation of China (NNSFC, 20604009 and 20774027), the Program for New Century Excellent Talents in University (for H. Ma, NCET-06-0413) and the Fundamental Research Funds for the Central Universities (WK0914042). All the financial supports are gratefully acknowledged. H. Ma also thanks the very kind donation of a Braun glove-box by AvH foundation.

Notes and references

- O. Dechy-Cabaret, B. Martin-Vaca and D. Bourissou, *Chem. Rev.*, 2004, **104**, 6147–6176.
- R. Mehta, V. Kumar, H. Bhumia and S. N. Upadhyay, *J. Macromol. Sci., Part C*, 2005, **45**, 325–349.
- N. E. Kamber, W. Jeong and R. M. Waymouth, *Chem. Rev.*, 2007, **107**, 5813–5840.
- R. H. Platel, L. M. Hodgson and C. Williams, *Polym. Rev.*, 2008, **48**, 11–63.
- H. Tsuji, F. Horii, S.-H. Hyonfand and Y. Ikada, *Macromolecules*, 1991, **24**, 2719–2724.
- H. Ma and J. Okuda, *Macromolecules*, 2005, **38**, 2665–2673.
- N. Spassky, M. Wisniewski, C. Pluta and A. L. Borgne, *Macromol. Chem. Phys.*, 1996, **197**, 2627–2637.
- C. P. Radano, G. L. Baker and M. R. Smith, *J. Am. Chem. Soc.*, 2000, **122**, 1552–1553.
- T. M. Ovitv and G. W. Coates, *J. Polym. Sci., Part A: Polym. Chem.*, 2000, **38**, 4686–4692.
- J. Zhong, Z. P. Dijkstra and J. Feijen, *Angew. Chem.*, 2002, **114**, 4692–4695.
- Z. Zhong, P. J. Dijkstra and J. Feijen, *J. Am. Chem. Soc.*, 2003, **125**, 11291–11298.
- M. H. Chisholm, J. C. Gallucci, K. T. Quisenberry and Z. Zhou, *Inorg. Chem.*, 2008, **47**, 2613–2624.
- Z. Tang, X. Chen, X. Pang, Y. Yang, X. Zhang and X. Jing, *Biomacromolecules*, 2004, **5**, 965.
- Z. Tang, X. Chen, Y. Yang, X. Pang, J. Sun, X. Zhang and X. Jing, *J. Polym. Sci., Part A: Polym. Chem.*, 2004, **42**, 5974–5982.
- Z. Tang, Y. Yang, X. Pang, J. Hu, X. Chen, N. Hu and X. Jing, *J. Appl. Polym. Sci.*, 2005, **98**, 102–108.
- X. Pang, H. Du, X. Chen, X. Zhuang, D. Cui and X. Jing, *J. Polym. Sci., Part A: Polym. Chem.*, 2005, **43**, 6605–6612.
- Z. Tang, X. Pang, J. Sun, H. Du, X. Chen, X. Wang and X. Jing, *J. Polym. Sci., Part A: Polym. Chem.*, 2006, **44**, 4932–4938.
- H. Du, X. Pang, H. Yu, X. Zhuang, X. Chen, D. Cui, X. Wang and X. Jing, *Macromolecules*, 2007, **40**, 1904–1913.
- N. Nomura, R. Ishii, Y. Yamamoto and T. Kondo, *Chem.–Eur. J.*, 2007, **13**, 4433–4451.
- H. Du, A. H. Velders, P. J. Dijkstra, Z. Zhong, X. Chen and J. Feijen, *Macromolecules*, 2009, **42**, 1058–1066.
- H. Ma, T. P. Spaniol and J. Okuda, *Dalton Trans.*, 2003, 4770–4780.
- C. Cai, A. Amgoune, C. W. Lehmann and J.-F. Carpentier, *Chem. Commun.*, 2004, 330–331.
- H. Ma, T. P. Spaniol and J. Okuda, *Angew. Chem., Int. Ed.*, 2006, **45**, 7818–7821.
- A. Amgoune, C. M. Thomas, T. Roisnel and J.-F. Carpentier, *Chem.–Eur. J.*, 2006, **12**, 169–179.
- X. Liu, X. Shang, T. Tang, N. Hu, F. Pei, D. Cui, X. Chen and X. Jing, *Organometallics*, 2007, **26**, 2747–2757.
- H. Ma, T. P. Spaniol and J. Okuda, *Inorg. Chem.*, 2008, **47**, 3328–3339.

- 27 R. H. Platel, A. J. P. White and C. K. Williams, *Chem. Commun.*, 2009, 4115–4117.
- 28 L. Clark, M. G. Cushion, H. E. Dyer, A. D. Schwarz, R. Duchateaub and P. Mountford, *Chem. Commun.*, 2010, **46**, 273–275.
- 29 C. K. Williams, L. E. Breyfogle, S. K. Choi, W. Nam, V. G. Young Jr., M. A. Hillmyer and W. B. Tolman, *J. Am. Chem. Soc.*, 2003, **125**, 11350–11359.
- 30 B.-H. Huang, C.-N. Lin, M.-L. Hsueh, T. Athar and C.-C. Lin, *Polymer*, 2006, **47**, 6622–6629.
- 31 Q. Dong, X. Ma, J. Guo, X. Wei, M. Zhou and D. Liu, *Inorg. Chem. Commun.*, 2008, **11**, 608–611.
- 32 V. Poirier, T. Roisnel, J.-F. Carpentier and Y. Sarazin, *Dalton Trans.*, 2009, 9820–9827.
- 33 M. Cheng, A. B. Attygalle, E. B. Lobkovsky and G. W. Coates, *J. Am. Chem. Soc.*, 1999, **121**, 11583–11584.
- 34 B. M. Chamberlain, M. Cheng, D. R. Moore, T. M. Ovitt, E. B. Lobkovsky and G. W. Coates, *J. Am. Chem. Soc.*, 2001, **123**, 3229–3238.
- 35 M. H. Chisholm, J. Gallucci and K. Phomphrai, *Inorg. Chem.*, 2002, **41**, 2785–2794.
- 36 J.-C. Wu, B.-H. Huang, M.-L. Hsueh, S.-L. Lai and C.-C. Lin, *Polymer*, 2005, **46**, 9784–9792.
- 37 M. H. Chisholm, J. C. Gallucci and K. Phomphrai, *Inorg. Chem.*, 2005, **44**, 8004–8010.
- 38 H.-Y. Chen, B.-H. Huang and C.-C. Lin, *Macromolecules*, 2005, **38**, 5400–5405.
- 39 H.-Y. Chen, H.-Y. Tang and C.-C. Lin, *Macromolecules*, 2006, **39**, 3745–3752.
- 40 Y. Huang, W.-C. Hung, M. Y. Liao, T. Tsai, Y. L. Peng and C.-C. Lin, *J. Polym. Sci., Part A: Polym. Chem.*, 2009, **47**, 2318–2329.
- 41 P. L. Arnold, I. J. Casely, Z. R. Turner, R. Bellabarba and R. B. Tooze, *Dalton Trans.*, 2009, 7236–7247.
- 42 M. H. Chisholm, J. C. Gallucci and H. Zhen, *Inorg. Chem.*, 2001, **40**, 5051–5054.
- 43 G. Labourdette, D. J. Lee, B. O. Patrick, M. B. Ezhova and P. Mehrkhodavandi, *Organometallics*, 2009, **28**, 1309–1319.
- 44 Y. Sarazin, R. H. Howard, D. L. Hughes, S. M. Humphrey and M. Bochmann, *Dalton Trans.*, 2006, 340–350.
- 45 In our unpublished work, when the alkyl-N(CH₃)₂ group is replaced with a methoxy group, the coordination of aryl-N(CH₃)₂ group to the zinc center is observed according to the molecular structure of an analogous zinc complex determined by X-ray diffraction.
- 46 M. Cheng, D. R. Moore, J. J. Reczek, B. M. Chamberlain, E. B. Lobkovsky and G. W. Coates, *J. Am. Chem. Soc.*, 2001, **123**, 8738–8749.
- 47 A. P. Dove, V. C. Gibson, E. L. Marshall, A. J. P. White and D. J. Williams, *Dalton Trans.*, 2004, 570–578.
- 48 M. P. Coles and P. B. Hitchcock, *Eur. J. Inorg. Chem.*, 2004, 2662–2672.
- 49 S. Groysman, E. Sergeeva, I. Goldberg and M. Kol, *Eur. J. Inorg. Chem.*, 2006, 2739–2745.
- 50 Z. Zheng, G. Zhao, R. Fablet, M. Bouyahyi, C. M. Thomas, T. Roisnel, O. C. Jr and J.-F. Carpentier, *New J. Chem.*, 2008, **32**, 2279–2291.
- 51 P. Hornmiron, E. L. Marshall, V. C. Gibson, A. J. P. White and D. J. Williams, *J. Am. Chem. Soc.*, 2004, **126**, 2688–2689.
- 52 W.-C. Hung and C.-C. Lin, *Inorg. Chem.*, 2009, **48**, 728–734.
- 53 In the absence of *rac*-lactide, the reaction of zinc complex **1** with one equiv. of isopropanol monitored with ¹H NMR spectroscopy however indicated partial decomposition of the complex to free ligand and “[Zn(OⁱPr)₂].” Complete decomposition to free ligand was further observed when two equiv. of isopropanol was added.
- 54 A. J. Chmura, M. G. Davidson, M. D. Jones, M. D. Lunn, M. F. Mahon, A. F. Johnson, P. Khunkamchoo, S. L. Roberts and S. S. F. Wong, *Macromolecules*, 2006, **39**, 7250–7257.
- 55 H. Bürger, W. Sawodny and U. Wannagat, *J. Organomet. Chem.*, 1965, **3**, 113–120.
- 56 G. Casiraghi, G. Casnati, G. Puglia, G. Sartori and G. Terenghi, *J. Chem. Soc., Perkin Trans. 1*, 1980, 1862–1865.
- 57 J. M. Lereestif, J. Perrocheau, F. Tonnard, J. P. Bazureau and J. Hamelin, *Tetrahedron*, 1995, **51**, 6757–6774.
- 58 C. Macleod, G. J. McKiernan, E. J. Guthrie, L. J. Farrugia, D. W. Hamprecht, J. Macritchie and R. C. Hartley, *J. Org. Chem.*, 2003, **68**, 387–401.
- 59 *SADABS*, Bruker Nonius area detector scaling and absorption correction, V2.05, Bruker AXS Inc., Madison, WI, 1996.
- 60 G. M. Sheldrick, *SHELXTL 5.10 for windows NT*, Structure Determination Software Programs, Bruker Analytical X-ray Systems, Inc., Madison, WI, 1997.
- 61 *SAINT*, Version 6.02, Bruker AXS Inc., Madison, WI, 1999.
- 62 G. M. Sheldrick, *SHELXS-97*, Program for the Solution of Crystal Structures, University of Göttingen, Germany, 1990.
- 63 G. M. Sheldrick, *SHELXL-97*, Program for the Refinement of Crystal Structures, University of Göttingen, Germany, 1997.
- 64 L. J. Farrugia, *J. Appl. Crystallogr.*, 1997, **30**, 565; *ORTEP-III for Windows-Version 2.0*, University of Glasgow, 2008.